

AD-A107 973

AIR FORCE INST OF TECH WRIGHT-PATTERSON AFB OH
AIRCRAFT POSITION MEASUREMENT USING LASER BEACON OPTICS.(U)
1981 S G WEBB

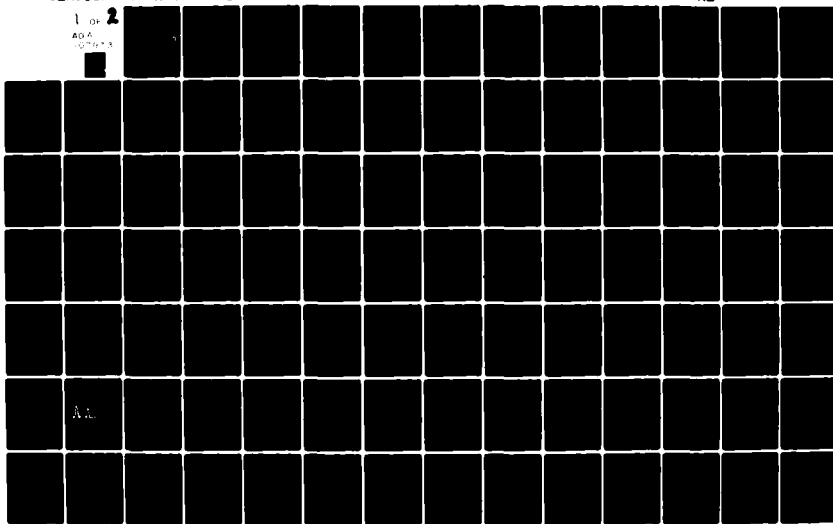
F/G 17/7

UNCLASSIFIED

AFIT-CI-81-58T

NL

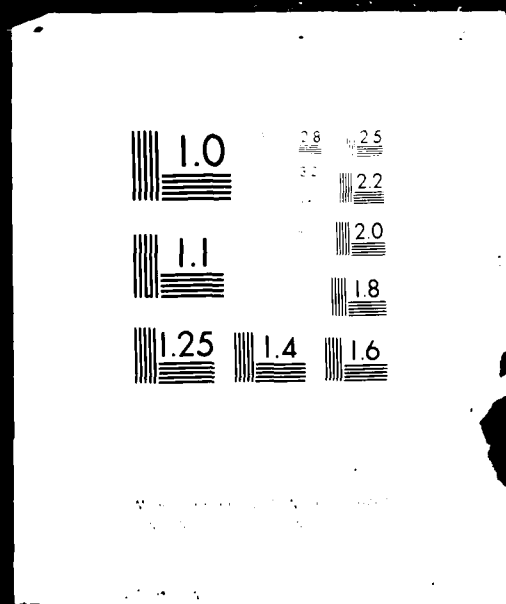
1 OF 2
ADA
107973



1 OF 2

AD A

107973



AD A 107973

ETIC FILE 7000

UNCLASS

SECURITY CLASSIFICATION OF THIS PAGE (When Data Entered)

REPORT DOCUMENTATION PAGE		READ INSTRUCTIONS BEFORE COMPLETING FORM
1. REPORT NUMBER 81-58T	2. GOVT ACCESSION NO. AD-A107 973	3. RECIPIENT'S CATALOG NUMBER
4. TITLE (and Subtitle) Aircraft Position Measurement Using Laser Beacon Optics		5. TYPE OF REPORT & PERIOD COVERED THESIS/DISSERTATION
7. AUTHOR(s) Steven G. Webb		6. PERFORMING ORG. REPORT NUMBER
9. PERFORMING ORGANIZATION NAME AND ADDRESS AFIT STUDENT AT: Princeton University		8. CONTRACT OR GRANT NUMBER(s)
11. CONTROLLING OFFICE NAME AND ADDRESS AFIT/NR WPAFB OH 45433		10. PROGRAM ELEMENT, PROJECT, TASK AREA & WORK UNIT NUMBERS
14. MONITORING AGENCY NAME & ADDRESS (if different from Controlling Office)		12. REPORT DATE 1981
LEVEL II		13. NUMBER OF PAGES 84
		15. SECURITY CLASS. (of this report) UNCLASS
16. DISTRIBUTION STATEMENT (of this Report) APPROVED FOR PUBLIC RELEASE; DISTRIBUTION UNLIMITED		15a. DECLASSIFICATION/DOWNGRADING SCHEDULE
17. DISTRIBUTION STATEMENT (of the abstract entered in Block 20, if different from Report) 23 NOV 1981		
18. SUPPLEMENTARY NOTES APPROVED FOR PUBLIC RELEASE: IAW AFR 190-17 <div style="text-align: right;"> <i>Fredric C. Lynch</i> FREDRIC C. LYNCH, Major, USAF Director of Public Affairs </div>		
19. KEY WORDS (Continue on reverse side if necessary and identify by block number) Air Force Institute of Technology (ATC) Wright-Patterson AFB, OH 45433		
20. ABSTRACT (Continue on reverse side if necessary and identify by block number) ATTACHED		

DD FORM 1 JAN 73 1473

EDITION OF 1 NOV 65 IS OBSOLETE

UNCLASS

SECURITY CLASSIFICATION OF THIS PAGE (When Data Entered)

81 11 30 003

AD A107973

DTIC FILE COPY

DTIC
ELECTE
DEC 1 1981
D

AFIT RESEARCH ASSESSMENT

The purpose of this questionnaire is to ascertain the value and/or contribution of research accomplished by students or faculty of the Air Force Institute of Technology (ATC). It would be greatly appreciated if you would complete the following questionnaire and return it to:

AFIT/NR
Wright-Patterson AFB OH 45433

RESEARCH TITLE: Aircraft Position Measurement Using Laser Beacon Optics

AUTHOR: Steven G. Webb

RESEARCH ASSESSMENT QUESTIONS:

1. Did this research contribute to a current Air Force project?
☐ a. YES ☐ b. NO
2. Do you believe this research topic is significant enough that it would have been researched (or contracted) by your organization or another agency if AFIT had not?
☐ a. YES ☐ b. NO
3. The benefits of AFIT research can often be expressed by the equivalent value that your agency achieved/received by virtue of AFIT performing the research. Can you estimate what this research would have cost if it had been accomplished under contract or if it had been done in-house in terms of manpower and/or dollars?
☐ a. MAN-YEARS ☐ b. \$
4. Often it is not possible to attach equivalent dollar values to research, although the results of the research may, in fact, be important. Whether or not you were able to establish an equivalent value for this research (3. above), what is your estimate of its significance?
☐ a. HIGHLY SIGNIFICANT ☐ b. SIGNIFICANT ☐ c. SLIGHTLY SIGNIFICANT ☐ d. OF NO SIGNIFICANCE
5. AFIT welcomes any further comments you may have on the above questions, or any additional details concerning the current application, future potential, or other value of this research. Please use the bottom part of this questionnaire for your statement(s).

NAME

GRADE

POSITION

ORGANIZATION

LOCATION

STATEMENT(s):

FOLD DOWN ON OUTSIDE - SEAL WITH TAPE

AFIT/NR
WRIGHT-PATTERSON AFB OH 45433

OFFICIAL BUSINESS
PENALTY FOR PRIVATE USE. \$300



NO POSTAGE
NECESSARY
IF MAILED
IN THE
UNITED STATES



BUSINESS REPLY MAIL

FIRST CLASS PERMIT NO. 73236 WASHINGTON D.C.

POSTAGE WILL BE PAID BY ADDRESSEE

AFIT/ DAA

Wright-Patterson AFB OH 45433

FOLD IN

AIRCRAFT POSITION MEASUREMENT USING LASER BEACON OPTICS

by

Steven G. Webb

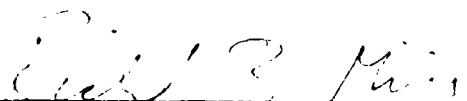
Princeton University
School of Engineering and Applied Science
Department of Mechanical and Aerospace Engineering

Submitted in partial fulfillment of the requirements for the degree
of Master of Science in Engineering from Princeton University, 1981

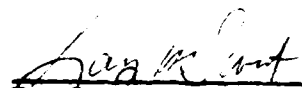
Prepared by:



Approved by:




Professor Richard B. Miles
Thesis Advisor



Professor Larry M. Sweet
Thesis Reader

I hereby declare that I am the sole author of this thesis.

I authorize Princeton University to lend this thesis to other institutions or individuals for the purpose of scholarly research.



Steven G. Webb

I further authorize Princeton University to reproduce this thesis by photocopying or by other means, in total or in part, at the request of other institutions or individuals for the purpose of scholarly research.



Steven G. Webb

Princeton University requires the signatures of all persons using or photocopying this thesis. Please sign below, and give address and date.

ABSTRACT

This thesis examines the development of a system to precisely measure the relative position between two aircraft in-flight utilizing a laser beacon, an optical detector array, and on-board microprocessing. As part of a cooperative research project with the NASA-Ames Research Center, the laser beacon system is designed to measure the range, azimuth, and elevation between a test helicopter and an observation aircraft, the YO-3A. The laser beacon board, mounted on the helicopter, consists of two orthogonal fan-shaped narrow width beams, which rotate at a constant four revolutions per second and have fields of view approaching 166 degrees. The beams sweep past an array of four optical detectors. Each detector is composed of two compound parabolic concentrators which collect the incoming laser beams over a 150 degree field of view, collimate the light so that the beams can pass through an interference filter, and then concentrate the laser beams on a photodiode. The photodiode transmits the detected beams, as pulses, to an electronics system where they pass through a band-pass filter and are converted into digital pulses for signal processing. The laser pulses are detected in the presence of background solar interference through optical spectral filtering of the incident light and electronic filtering of the photodiode signal.

Accession For	
NTIS	SPAAI
DTIC TAB	
Unannounced	
Justification	
By	
Distribution	
Availability	Audio
Dist	Avail and/or
	Special
A	

Initial tests of the laser beacon and the detector optics have demonstrated the potential for their use as elements of a relative position measurement system.

ACKNOWLEDGEMENTS

The author wishes to express his sincere gratitude to Professor R. B. Miles and Professor L. M. Sweet for their continual advice and encouragement during this project. Invaluable technical assistance was provided by Mr. G. Cutso-george, Mr. E. Griffith, Mr. G. Russell, and Mr. E. Wong. Tuition for the author was generously provided for by the Guggenheim Fellowship Foundation, and the U. S. Air Force graciously granted a year's leave of absence in order to complete this Master's Degree. This research project has been sponsored by the NASA-Ames Research Center under Grant NCC 2-94.

This thesis carries 1535-T in the records of the Department of Mechanical and Aerospace Engineering.

TABLE OF CONTENTS

ABSTRACT	iv
ACKNOWLEDGEMENTS	vi

<u>Chapter</u>	<u>page</u>
I. INTRODUCTION	1
II. LASER BEACON	8
Introduction	8
Beacon Design	9
Laser Characteristics	9
Reflecting Mirror	12
Beacon Description	14
Testing and Modifications	24
Field of View Testing	24
Rotation Accuracy Testing	28
Summary	30
III. DETECTOR OPTICS	31
Introduction	31
Detector Design	31
Spectral Filtering	32
Detector Optics	33
CPC Design	36
Testing and Modifications	43
Lens System	43
CPC Detector System	45
Summary	51
IV. DETECTOR ELECTRONICS	52
Introduction	52
Package Design	52
Electronic Filters	52
Threshold and Gain Adjustment	56
Electronic Components	57
Summary	62
V. DETECTOR ARRAY	63
Introduction	63
Two-Dimensional Position Calculation	64

Three-Dimensional Position Calculation	66
Fundamentals of the Array Design	73
Two-Detector Testing	74
Array Construction	79
Summary	80
VI. CONCLUSIONS	81
REFERENCES	83
<u>Appendix</u>	<u>page</u>
A. DERIVATION OF THE POSITION DETERMINATION EQUATIONS	84

LIST OF TABLES

<u>Table</u>	<u>page</u>
1. Beam Widths, Depths of Focus, and Intensities for Three Different Source Widths and a $\Delta\alpha$ Equal to 120 Degrees	11

LIST OF FIGURES

<u>Figure</u>	<u>page</u>
1. Aircraft Positioning for Measurement Acquisition . . .	3
2. Schematic of Laser Beacon System	6
3. Laser Beacon Layout	15
4. Distance Between Lenses as a Function of Range for Various Minimum Beam Widths and an 18° Cone Angle Expanding Lens	19
5. Incident Laser Light Reflected by a Cylindrical Mirror	20
6. Laser Beacon Mounting Configuration	23
7. Isolator Mounting Configuration	24
8. Laser Beacon Blind Spots Caused by a Lens Mount Obstructing its Own Laser Beam	25
9. Laser Beacon Blind Spots Caused When One Set of Lens Mounts Obstructs the Laser Beam From the Other Lens Mounts	26
10. Beacon Orientation for a 166 Degree Field of View .	27
11. Beacon Orientation for a 148 Degree Field of View .	27
12. Mean Value and Error for Beacon Motor With and Without a Belt Drive	29
13. Model of a Wide Angle Collector Consisting of a Reflecting Ball and a Collimating Lens	35
14. CPC Detector Design, Consisting of Two CPCs and an Interference Filter	38
15. CPC Geometry, With Light Entering Aperture d Over a Wide Field of View and Exiting Aperture D as a "Collimated" Beam	40

16.	CPC Length Versus Exit Divergence Angle for Varying Fields of View and Varying Exit Aperture Diameters	42
17.	F 1 Lens Collector System Consisting of Two Plano- Convex Lenses and an Interference Filter	44
18.	Intensity Versus Incidence Angle Without Interference Filters for Both a Standard CPC and a CPC With a Bit Cut Off	47
19.	Normalized Intensity With a) No Interference Filter, b) a 10 Angstrom Filter, and c) a 30 Angstrom Filter	49
20.	Gaussian Laser Beam Signal and its Fourier Transform	55
21.	Stages of the Electronic Pulse as it is Processed From a Raw Photodiode Signal to the Final Digital Pulse Form	56
22.	Schematic of the Electronics System	59
23.	Schematic of the Signal Processor	60
24.	Schematic of the Sensor and the Preamplifier	60
25.	Bode Plot of the Measured Response of the Electronics System	61
26.	Two-Dimensional Geometry for Relative Position Calculations	66
27.	A Four Detector Array	67
28.	Three-Dimensional Geometry for Relative Position Calculations	70
29.	Lateral Beacon Sweeps With and Without a Roll Angle	71
30.	Laser Beam Plane Geometry for Relative Position Calculations	73
31.	Plot of Time Interval Errors from the Mean as a Function of the Separation Distance Between Two Detectors	75
32.	Plot of Time Interval Errors from the Mean as a Function of the Detector Incidence Angle to the Beacon Axis	78
33.	Detector Array Configuration	85

34.	Beam Plane Geometry for Relative Position Calculations	86
35.	Plane Distance Geometry for Relative Distance Calculations	89

Chapter I

INTRODUCTION

This thesis considers the development of the techniques and the hardware required for the laser beacon position measurement system which is to be used in conjunction with a NASA-Ames research project.

The NASA-Ames Research Center and the U. S. Army Aeromechanics Laboratory are currently involved with experiments to obtain in-flight acoustics measurements of radiated noise from helicopters in the far-field. Their aim in making these measurements is to validate theory for blade-vortex interactions and other mechanisms of helicopter noise [1].

NASA and the Army are examining four different two-bladed rotors with respect to their blade-vortex interactions and collating the results. The UH-1H helicopter is being tested with the standard NACA 0012 airfoil rotor, while the AH-1S helicopter is being tested with its 540 rotor as well as the Kaman K747 rotor and the OGEE tip rotor. With the various rotors, the research group proposes to generate blade-vortex interaction impulsive noise by means of the interaction of a rotor blade with previously generated tip vortices. Usually, these measurements have been acquired with ground-based methods.

However, relative motion, ground reflection, and other effects due to gathering data this way are minimized if in-flight, far-field measurement techniques to gather the information are utilized. With this new method, the helicopter with the rotor to be tested is positioned visually with respect to a fixed wing aircraft--for the experiments, a YO-3A is employed--carrying microphones and recording equipment (figure 1). The YO-3A flies a pre-determined course, and noise measurements are taken with the helicopter behind the plane in a variety of flight positions.

While this method of gathering blade-vortex interaction data is superior to the other methods used, the relative position between the aircraft and the helicopter is not precisely known. As a result, during the analysis of the acquired data an error is unavoidably introduced.

Consequently, NASA and the Army require a precise method of gathering very accurate position information for simultaneous recording with the measured noise. In addition, they desire a system of displays to assist the helicopter pilot and the flight engineer on board the YO-3A in maintaining specified relative positions under different flight conditions.

The objective of the research program at Princeton University is to develop techniques for accurately measuring the precise relative position between the helicopter and the YO-3A utilizing a laser beacon system, a detector array, and

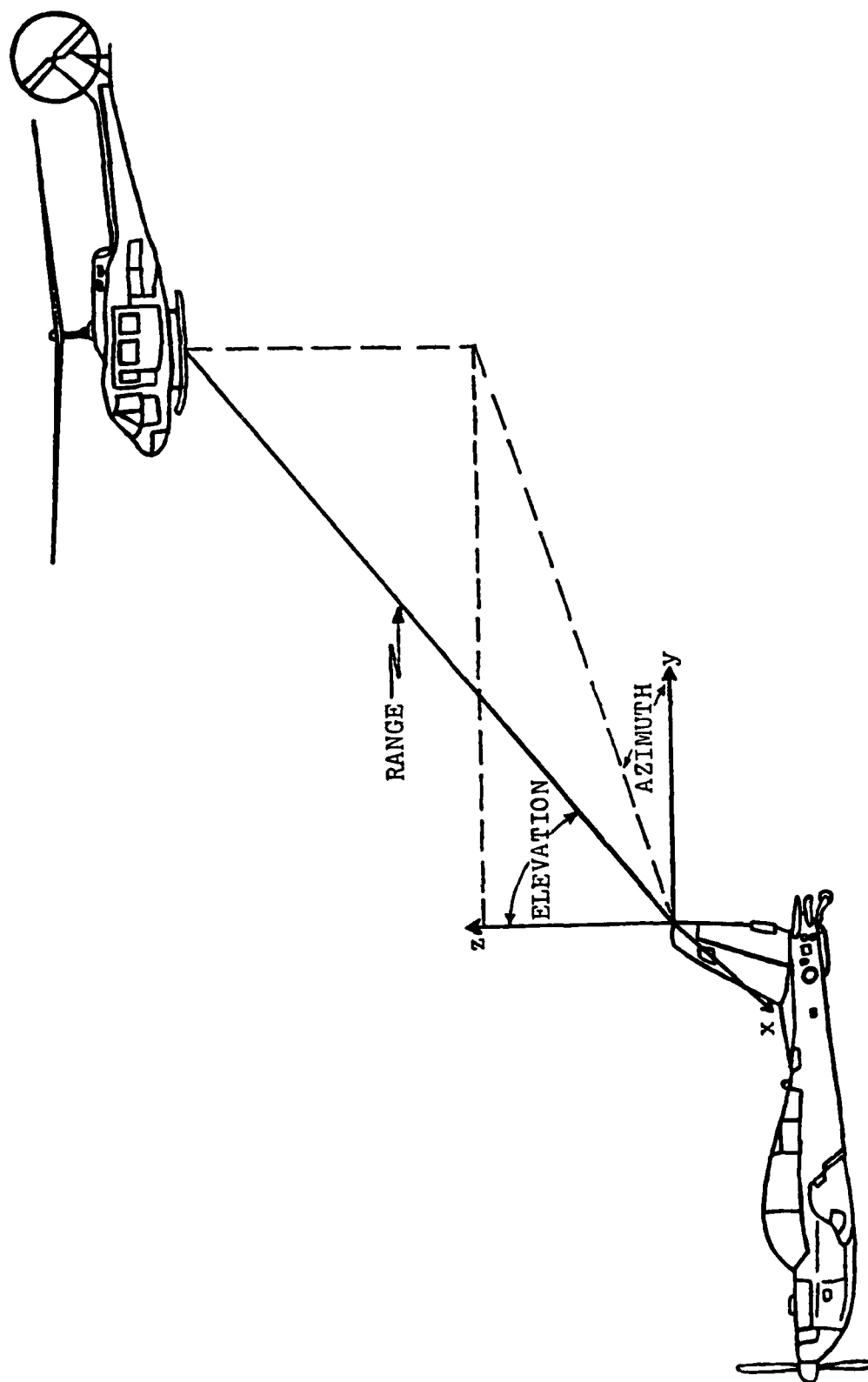


Figure 1: Aircraft Positioning for Measurement Acquisition

on-board microprocessors. The specific application of this system will constitute measuring not only the distance between the two aircraft, but also the relative elevation and azimuth angles. The design goals are to attain a range accuracy of better than 0.5 percent while maintaining the elevation and azimuth angles to within an accuracy of one degree.

The research for the laser beacon project was initiated by Profesor R. B. Miles in 1978 with respect to developing a laser/optics system for application in general aviation aircraft collision warning. Professor Miles [2] made theoretical calculations of the extent to which a laser beacon system is range sensitive under both ideal and non-ideal atmospheric conditions. In addition, he obtained experimental results indicating that accurate range measurements were feasible in daylight conditions with substantial atmospheric scintillation. In 1980, Professor Miles, along with Professor L. M. Sweet, obtained a contract from the U. S. Army and the NASA-Ames Research Center to develop a relative position measurement system using a laser beacon system.

The system developed under this contract (see figure 2) consists of collimated beams of low-power HeNe laser light that are reflected from rotating cylindrical mirrors, forming a fan-shaped laser beacon centered at the source aircraft--the helicopter being tested. An array of optical detectors on board the target aircraft--the YO-3A--senses the

beam sweeps, and the subsequent real-time computer processing of the detected signals yields information on the aircrafts' relative linear and angular positions. This processed data is then sent to the on-board tape recorder to be used in conjunction with the collected noise data. In addition, the data is sent to displays for the helicopter pilot and the flight engineer on board the YO-3A.

This thesis will concentrate on the development of the laser beacon, the detector optics and associated electronics, and the detector array. Issues to be addressed include:

a) Beacon Optics: designed for precise position measurements, important considerations include the following:

- i) laser frequency
- ii) collimation
- iii) focusing
- iv) field of view
- v) speed and precision of the beacon rotation

b) Detector Optics and Electronics: design the detectors and electronics with respect to:

- i) wide angle viewing
- ii) spectral filtering
- iii) electronic filtering
- iv) processed signal to microprocessor

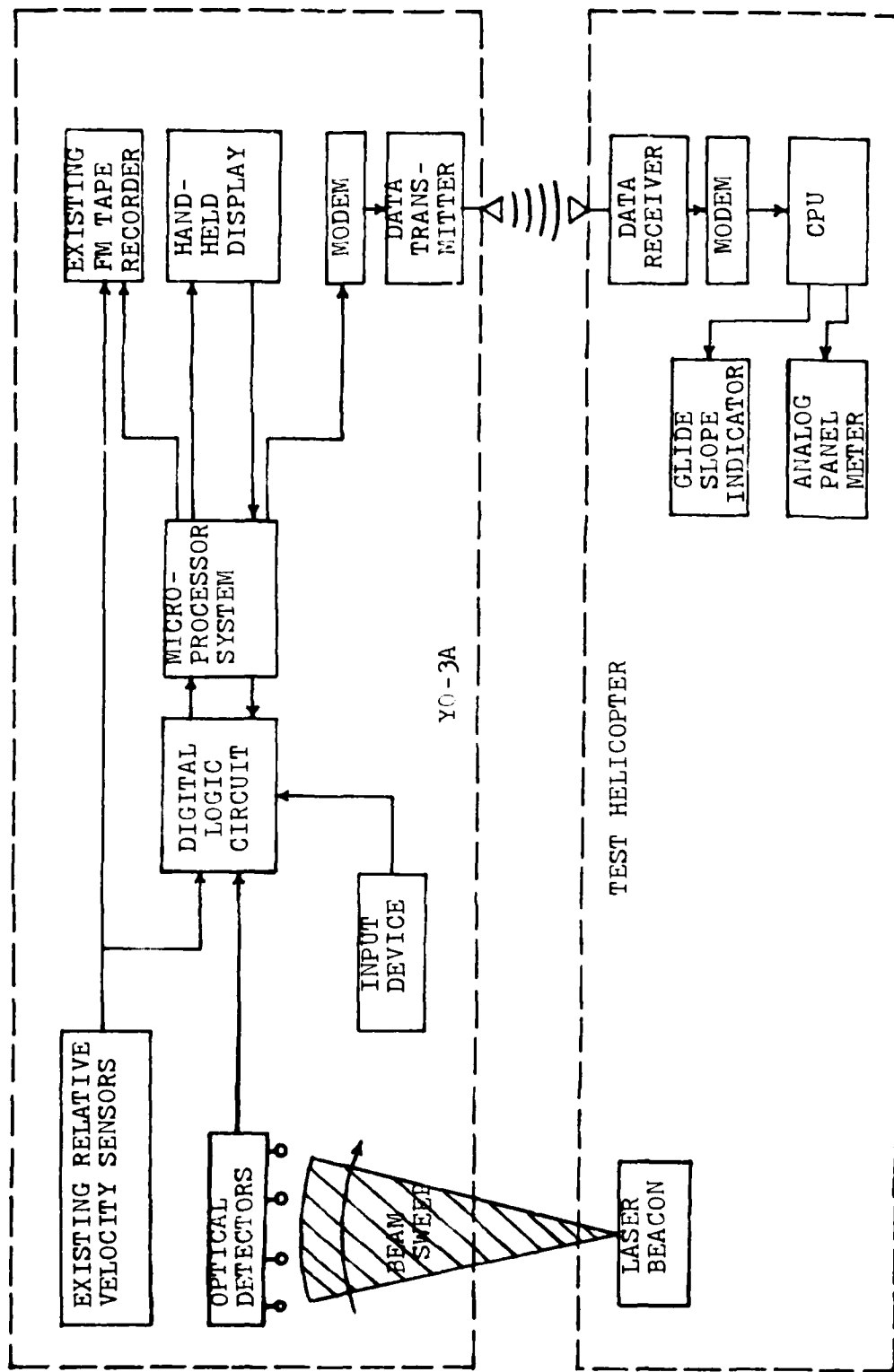


Figure 2: Schematic of Laser Beacon System

c) Detector Array: consider influencing factors such as:

- i) weight
- ii) size
- iii) shadowing
- iv) field of view
- v) range and angle sensitivity

Chapter II

LASER BEACON

2.1 INTRODUCTION

The purpose of the laser beacon is to generate narrow width laser beams which sweep past a detector array and are sensed by each detector in a variety of flight positions. Since it is to be mounted on the helicopter's nose, the beacon needs to be designed and built as rugged and as simply as possible in order to withstand any vibrations or other disturbances created by the helicopter. In addition, the beacon size should be minimized for convenient packaging on board the helicopter. The laser must be low power in order to minimize cost, power utilization, and prevent the possibility of constituting any hazard to the eye. Operating off the helicopter's 28 volt power supply, the beacon needs to provide constant rotation frequency narrow width laser beams to be swept about two orthogonal axes in order to provide three dimensional position measurements. Finally, the system must cover the better part of a hemisphere in order to accommodate the wide range of positions to be assumed by the helicopter relative to the YO-3A.

2.2 BEACON DESIGN

2.2.1 Laser Characteristics

A laser was chosen as the source for the beacon system in order to allow for strong discrimination against sunlight and to create the required beam profile. The system utilizes the laser's optical properties of narrow spectral width and spatial coherence.

For the design, and for possible use as a collision warning system, a five milliwatt continuous wave helium-neon laser, operating in the red portion of the spectrum at 6328 Angstroms, was selected. The laser beam is focused at a nominal range of 30 meters--the operating distance between the two aircraft. There is a tradeoff between the beam width and the distance from the source. Specifically, due to the principles of diffraction, for a beam with a gaussian profile, the minimum beam width, w , at a distance, R , from a source can be expressed as

$$w(R) = \frac{4 \lambda R}{\pi w_0}$$

where w_0 is the width between the $1/e^2$ intensity points at the source ($R=0$), and λ is the laser wavelength

If the laser beam has a horizontal width w_0 at the source and is allowed to diverge in the vertical plane at a con-

stant angle $\Delta\alpha$ between the $1/e^2$ intensity points, then the maximum intensity at distance R is [2]

$$I(\alpha, \gamma) = I_0 \exp\left[-\frac{8\alpha^2}{(\Delta\alpha)^2}\right] \exp\left[-\frac{8\gamma^2 R^2}{w^2(R)}\right]$$

where

$$I_0 = \frac{8P}{\pi R w(R) \Delta\alpha \exp\left[-\frac{(\Delta\alpha)^2}{32}\right]}$$

and P is the total laser power

γ is the azimuth angle of the beam in radians, assuming that γ equals zero at the beam center line and the beam has a gaussian profile

α is the angle from the horizontal plane in radians

Thus, if a five milliwatt laser is focused at several ranges for three different source widths-- w_0 in the horizontal direction is 5 mm in one case, 1 cm for the second, and 3 cm in the third case--and $\Delta\alpha$ is 120 degrees (the beam is expanded plus or minus 60 degrees about the vertical axis), then the minimum beam widths and the maximum center intensities for the different ranges are shown in Table 1. Due to diffraction, at large distances the minimum beam width is larger than the beam width at the source. Increasing the source beam width decreases the minimum beam width achievable, and, consequently, increases the maximum center

intensity. Thus, the highest intensity, which leads to the best detectability, requires a large source beam width. In addition, this emphasizes the point that focusing at the nominal range is critical.

TABLE 1

Beam Widths, Depths of Focus, and Intensities for Three Different Source Widths and a $\Delta\alpha$ Equal to 120 Degrees

$R (m)$ $w_o (m)$		10	30	100
5×10^{-3}	$w (m)$	1.611×10^{-3}	4.834×10^{-3}	1.611×10^{-2}
	$b (m)$	2.268	1.090×10^1	4.085×10^1
	$I_o (\frac{\text{watt}}{m^2})$	4.328×10^{-1}	4.809×10^{-2}	4.328×10^{-3}
1×10^{-2}	$w (m)$	8.057×10^{-4}	2.417×10^{-3}	8.057×10^{-3}
	$b (m)$	7.412×10^{-1}	5.584	3.470×10^1
	$I_o (\frac{\text{watt}}{m^2})$	8.655×10^{-1}	9.617×10^{-2}	8.655×10^{-3}
3×10^{-2}	$w (m)$	2.686×10^{-4}	8.057×10^{-4}	2.686×10^{-3}
	$b (m)$	8.872×10^{-2}	7.841×10^{-1}	8.157
	$I_o (\frac{\text{watt}}{m^2})$	2.597	2.885×10^{-1}	2.597×10^{-2}

Related to the beam focusing is the laser's depth of focus. There exists a tradeoff between the beam width w at the focus and the distance over which w is to be maintained. In other words, the depth of focus, δ , is dependent upon the

width desired. The wider the focus depth, the larger the beam width. For a given source beam width, w_0 , the depth of focus, δ , is the distance beyond a range, R , to a point, R , such that, at R , the beam is focused to the minimum beam width, w , and the beam diverges until, at R , the beam has a width $\sqrt{2} w$. This depth of focus can be expressed as

$$\delta = \left[\frac{-R + R\sqrt{2 + A^2}}{1 + A^2} \right]$$

where

$$A = \frac{\pi w_0^2}{4 \lambda R}$$

The influence that the beam width has on the depth of focus affects the accuracy of the measured sweep rate at positions other than the prescribed nominal range. In turn, this affects the accuracy of the position measurements. Table 1 illustrates the effects of width on the focus depth.

2.2.2 Reflecting Mirror

In order to permit an angular divergence approaching 180 degrees while at the same time minimizing the beam width so that it is easier for a detector to sense a beam sweep, a cylindrical mirror is utilized. This mirror reflects the collimated light in a fan-shaped beam in the vertical axis.

When focused at some nominal range, this fan-shaped beam has a narrow width in the horizontal axis.

The mirror must rotate at a constant speed in order to provide a high degree of accuracy in position measurements. The rotation rate must be fast enough to allow for frequent updating of the range, elevation, and azimuth between the YO-3A and the helicopter. However, the rate cannot be too rapid, or the detector electronics will not detect the beam sweeps. Since the observed sweep velocity, v , is proportional to range, R , a relationship can be derived.

$$v = 2\pi R/\Delta t$$

where Δt is the number of seconds required to complete a full beam sweep (period of rotation)

This result implies that the range accuracy is limited to the accuracy of the rotation rate.

One rotating cylindrical mirror yields two-dimensional position measurements in a plane--that is, the distance between the detectors and the rotation axis of the laser beacon, and the direction of the travel vector defined by the perpendicular to the light plane. This restricts the mirror's sweep axis to lie tangent to a circle (with the mirror at the origin and the radius being defined as the distance between the aircraft) and in the plane perpendicular to the travel vector. Consequently, an additional beam is required

to obtain three-dimensional position measurements. The laser beacon therefore needs to have two orthogonal beams that sweep across the detector array. The rotating reflectors should be synchronized to be 180 degrees out of phase so that the two beams will never coincide.

2.2.3 Beacon Description

Based on the preceding requirements for the laser beacon, a design was drafted and a prototype beacon has been constructed (figure 3).

The design centers around two separate lasers which shine on orthogonal reflecting mirrors. A one-laser beacon was considered, but complexities in accurately gearing and synchronizing a beam splitter led to the consensus that, in the long run, a two-laser beacon would probably be simpler to construct and yield more accurate results.

The lasers are secured to the beacon's lower surface, and the laser beams are reflected to the upper surface by prisms. An expanding lens and condensing lens arrangement is used to expand each beam to a specific source width and focus the beam at the desired nominal range. The expanding lens expands the beam after exiting the laser source. Adjusting the condensing lens attains the minimum beam width at the desired operating distance. Secured to the beacon's upper surface, two separate sets of lenses are used--one set for each laser.

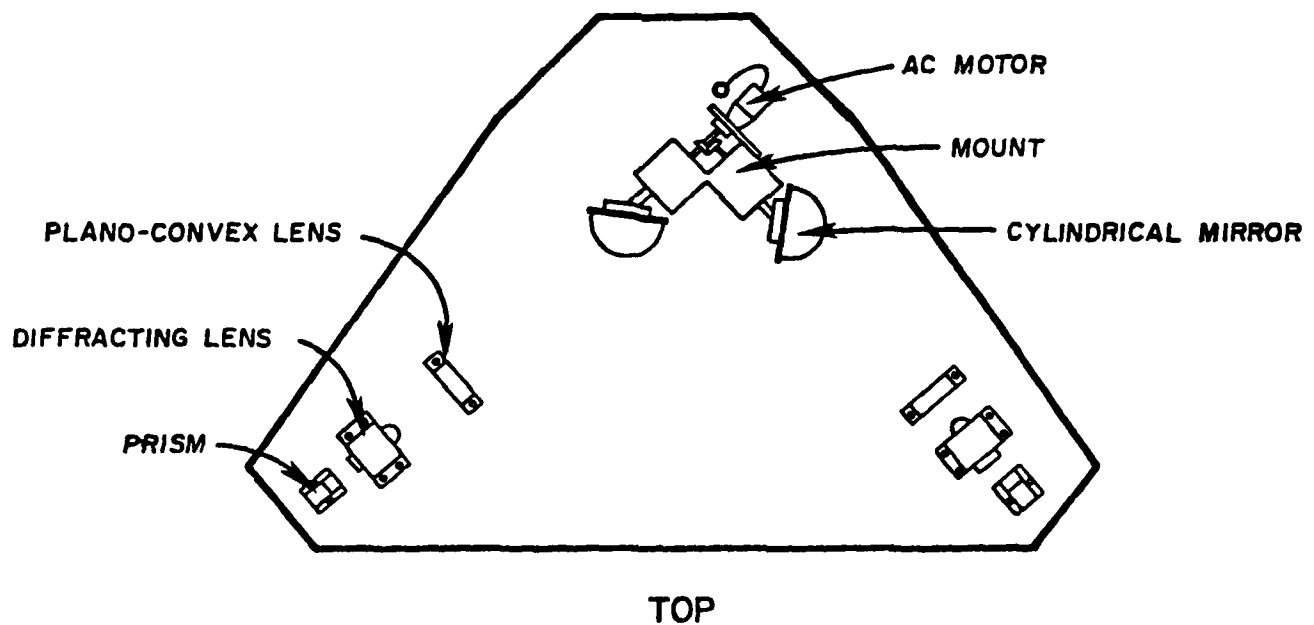
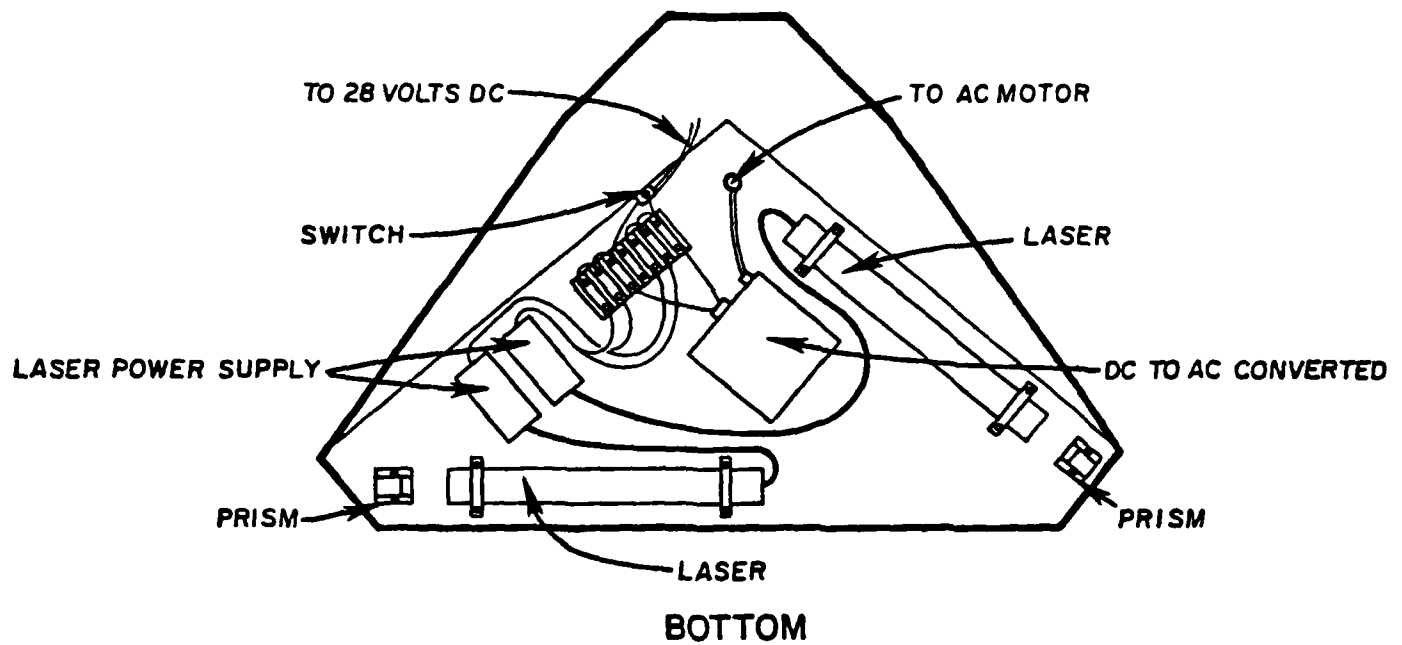


Figure 3: Laser Beacon Layout

The source beam width is optimized in order to attain both the maximum intensity and the smallest practical beam width at the nominal range. For a 30 meter range and a 0.56 mm diameter width at the focus, the calculated source beam width is 43 mm. It should be noted that, due to effects such as atmospheric scintillation, the focused beam width at the 30 meter range will be larger than 0.56 mm. The expanding lens has been chosen based upon the concept of maximizing the beam intensity while minimizing the distance between the two lenses. A 60X microscopic objective lens was utilized for the experiments. The microscopic objective lens is approximately an $f\ 1$ lens (where the f number is defined as being the ratio of the lens' focal length to its diameter), which means that its diameter approximately equals its focal length. The maximum expansion cone angle of an $f\ 1$ lens is 53 degrees. In order to minimize distortion, the laser illuminates only the center portion of the lens, and the beam is expanded about a cone angle of 18 degrees. The condensing lens is chosen to have approximately the same diameter as the calculated source beam width to minimize interference with the beacon. The focal length of the condensing lens approximately equals the distance between the two lenses when the beam is focused at the desired nominal range.

The distance between the condensing lens and the expanding lens places constraints on the size of the beacon appa-

ratus. As can be seen in figure 4, for a given expansion lens (a 60X microscopic objective lens is used in this case) and a specific focused minimum beam width, the distance between the two lenses varies with the nominal range. In order to achieve a constant focused minimum beam width with increasing range, both the source beam width and the distance between the two lens must be increased. This can be a factor if future applications of the beacon require small beacon sizes, tightly focused beams, and large operating distances.

The minimum beam width is constrained by the source beam width and the desired range. The distance between the expanding lens and the condensing lens cannot be smaller than the focal length of the condensing lens. Generally, the f number of the condensing lens is matched to the expansion cone angle of the chosen expanding lens. Likewise, the focal length of the condensing lens cannot be smaller than the source beam width, since the best expansion lenses available have f numbers equal to one. Thus, referring to figure 4, the hash marks on each of the lines, indicating the various minimum beam widths, dictates this lower limit. The only other restriction is that the diameter of the condensing lens must be greater than the source beam width so that all of the incident laser light is able to pass through the lens. For this research project, the condensing lens used is a plano-convex lens with a 40 mm diameter (which is

matched to the source beam width to eliminate blind spots) and a focal length of 150 mm.

The size of the laser beacon used in this project is constrained by the particular configuration chosen. Examining the beacon layout reveals the fact that the beacon is set up in a right isosceles triangular configuration. For the most practical configuration, the length of each of the beacon's sides is greater than the length of each laser. Figure 4 illustrates the wide range of distances between the two lenses which can be achieved when the distance between the lenses is constrained to be less than the length of the laser and the lens mounts. Beacons not constrained in this manner will have different size limitations.

After passing through the condensing lens, the laser light is then expanded into a fan-shaped beam by the cylindrical mirror. The mirror's size is chosen such that all incident light is reflected by a 90 degree cylindrical segment on the mirror (see figure 5). The mirrors actually used have 120 degree segments to allow for mounting and safety margins when they reflect the incident light. Thus, the widest possible divergence can be attained with negligible light loss.

A synchronous motor, attached to the upper surface of the beacon, drives the two reflecting mirrors. The mirror axes are orthogonal to each other and rotate 180 degrees out of phase. In order to optimize the revolution rate to attain a

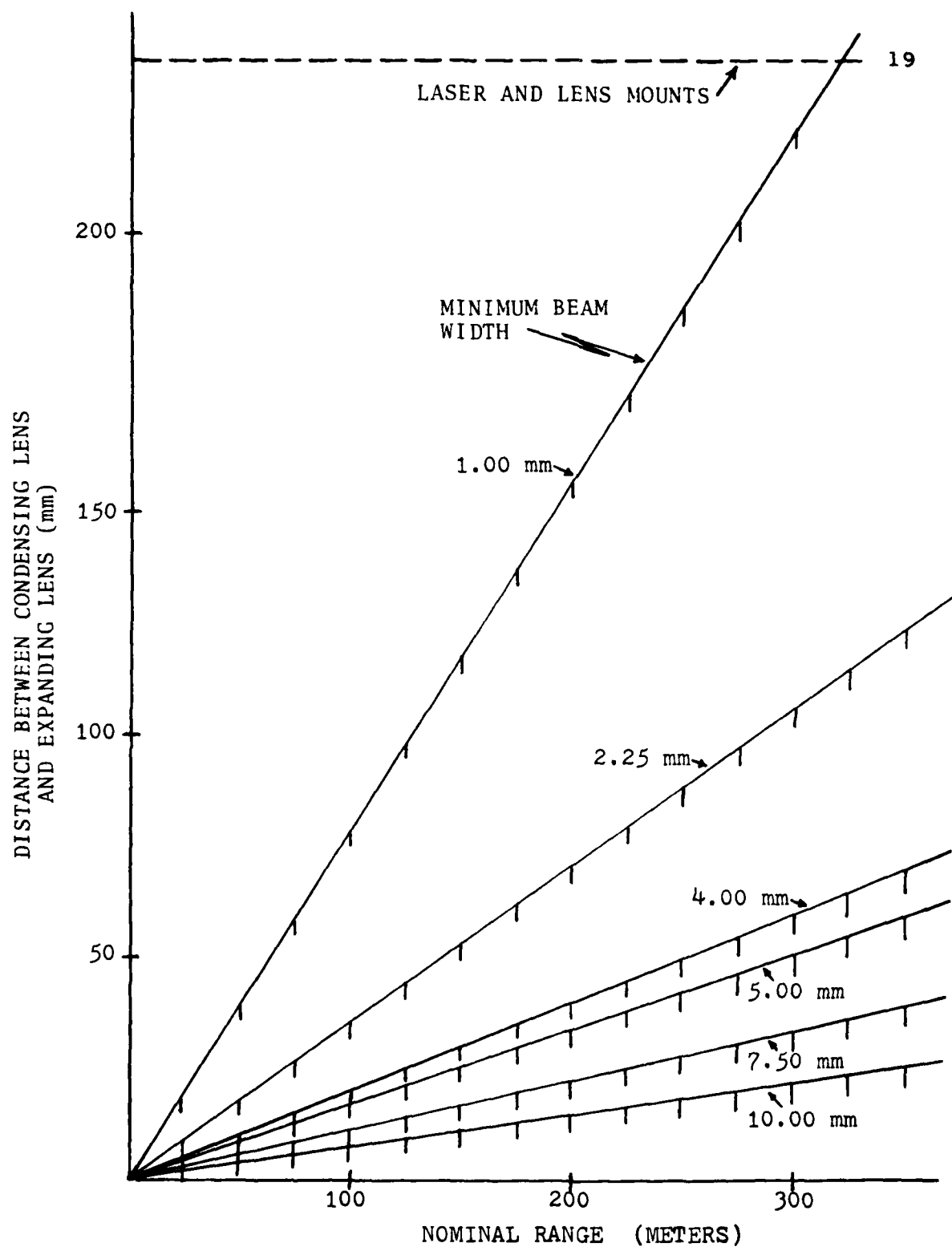


Figure 4: Distance Between Lenses as a Function of Range for Various Minimum Beam Widths and an 18° Cone Angle Expanding Lens

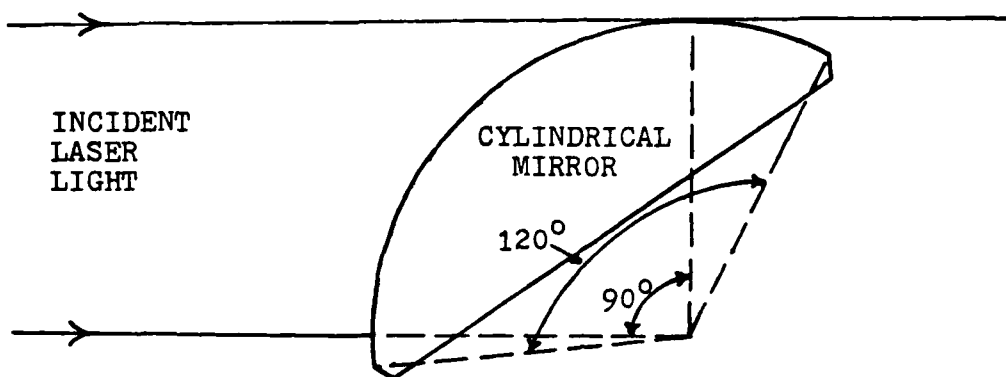


Figure 5: Incident Laser Light Reflected by a Cylindrical Mirror

high number of position updates without degrading the integrity of the system, the motor runs at a constant four revolutions per second.

The lasers and the motor are powered by the helicopter's 28 volt DC power supply. Commercial power supplies rated at this voltage operate the lasers. However, the need for a synchronous motor dictates the use of a 400 cps DC/AC power converter.

Since the laser beacon is to be mounted on the nose of a helicopter and subjected to various vibration modes, all pieces of equipment on the beacon are rigidly fastened to a thick base plate. This aids in maintaining alignment during operation. In order to protect the mirrors and the lenses, a glass plate will be placed on the beacon's upper surface.

Isolation mounts will be used to isolate the laser beacon from the helicopter's vibrations. The major vibrations on the nose of the helicopter are due to lateral and vertical excitations from both the rotor hub and the tail stinger, and occur in the frequency range between 3 and 40 Hz. Harmonics above 40 Hz are negligible. Perfect isolation, which eliminates all vibration frequencies, is not practical since at very low frequencies the isolators are extremely soft and may not properly support the expected loads. Examining the helicopter's frequency responses shows that most of the vibrations occurring between 3 and 40 Hz are above 15 Hz. Consequently, the optimum isolator should damp out vibrations above 15 Hz. However, the dynamic natural frequencies of each isolator must not match the helicopter's 2/rev and 4/rev excitation frequencies or the resonances will be excited. Therefore, the isolator dynamic responses in yaw, pitch, and roll should be calculated to insure that none of the resonances will be excited.

The primary forces exerted on the beacon are due to gravity and drag. Thus, isolators eliminating vibrations above 15 Hz are chosen to support the beacon under both the compression and the shear forces expected.

NASA desires the helicopter to conduct tests from ten degrees below the YO-3A's horizontal plane to 90 degrees above the plane. To provide the laser beacon with a field of view covering this range of positions, the beacon will be mounted

at an inclination angle of 45 degrees. (see figure 6). Sixteen sandwich mounts--six to support the load in compression and ten for shear support--will be used to maintain vibration isolation (see figure 7). The isolators are calculated to damp out vibrations above 16.64 Hz caused by the anticipated compression forces and vibrations above 12.42 Hz caused by the shear forces. The various dynamic natural frequencies calculated for the selected isolator mounting configuration are: 12.56 Hz and 24.20 Hz in the roll mode; 19.80 Hz and 24.20 Hz in the pitch mode; and 13.56 Hz and 16.08 Hz in the yaw mode. These resonances do not match the expected excitation frequencies. For example, the UH-1H main rotor (324 rpm, 2 blades) has the closest 2/rev (10.8 Hz) and 4/rev (21.6 Hz) excitation frequencies.

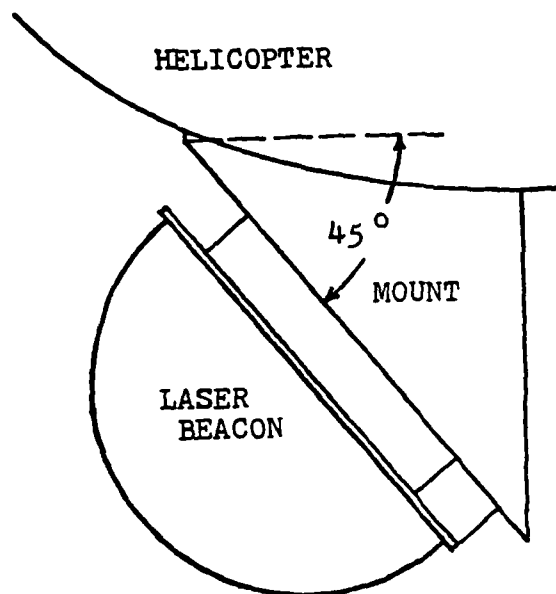


Figure 6: Laser Beacon Mounting Configuration

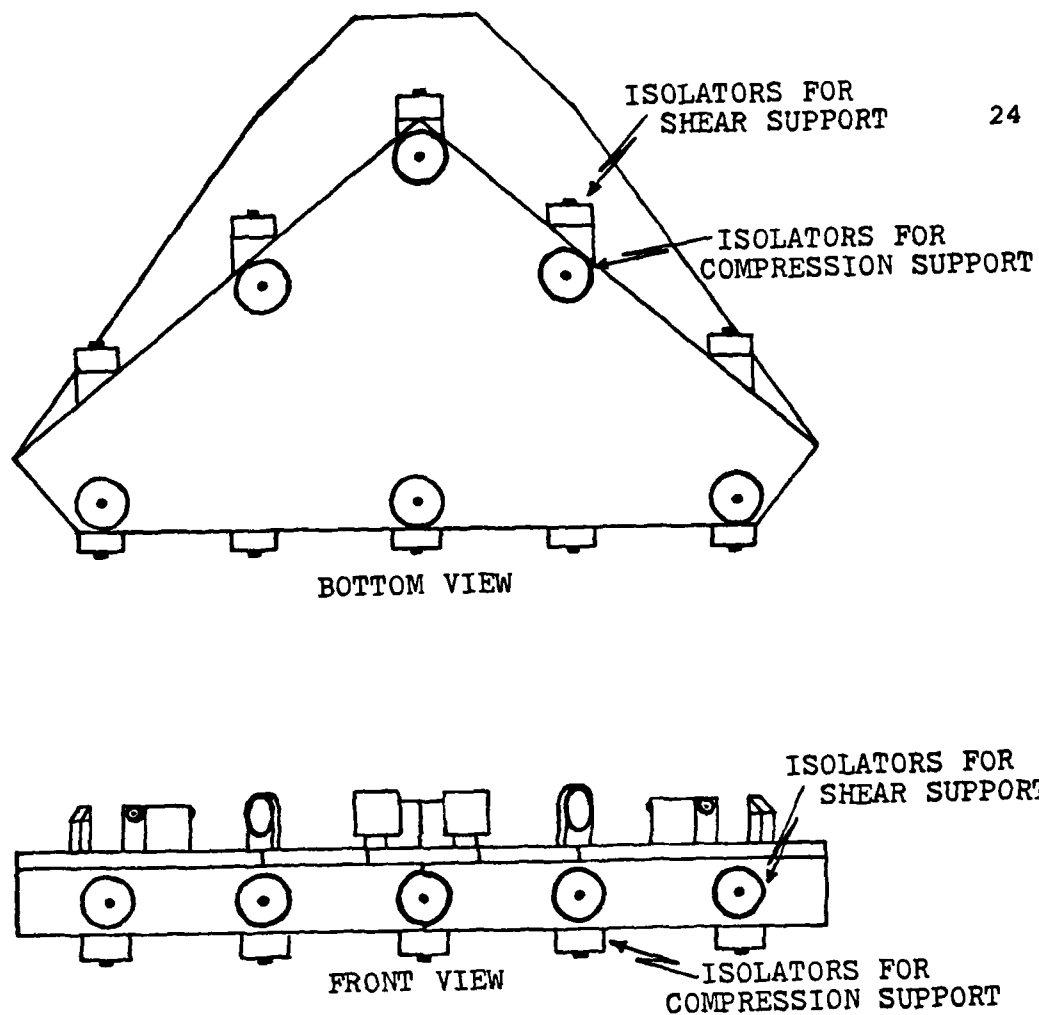


Figure 7: Isolator Mounting Configuration

2.3 TESTING AND MODIFICATIONS

2.3.1 Field of View Testing

For testing purposes, all measurements were made without the glass plate in place. The laser beacon possessed two narrow width beams which were focused 30 meters downrange with angular divergences approaching 166 degrees.

The beacon has four blind spots near the edge of the field of view due to lens mount obstructions. The first blind spot occurs when one set of the lens mounts is between the detector and the beam emanating from that particular lens set (see figure 8). In this case, although one laser beam is totally obscured by the mounts, the other beam is still visible. The second blind spot is identical to the first, only this time the blind spot is due to the other set of lens mounts.

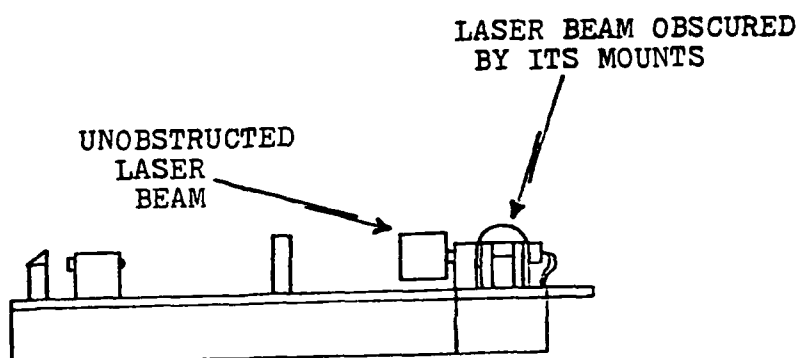


Figure 8: Laser Beacon Blind Spots Caused by a Lens Mount Obstructing its Own Laser Beam

The third blind spot occurs when one laser beam is obstructed by the other beam's (whose field of view remains visible) lens mounts and reflecting mirror (see figure 9). The final blind spot occurs on the opposite side of the beacon in a manner similar to the third blind spot.

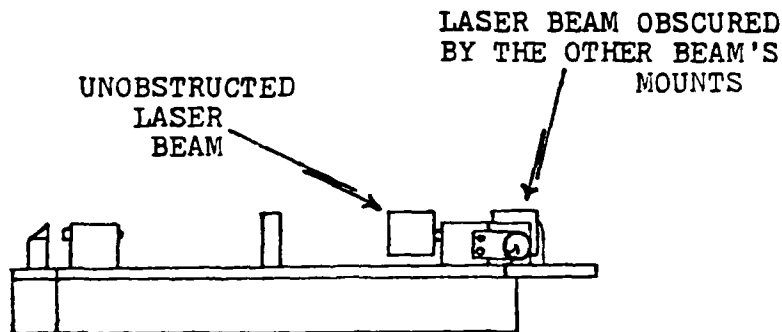


Figure 9: Laser Beacon Blind Spots Caused When One Set of Lens Mounts Obstructs the Laser Beam From the Other Lens Mounts

In between the two sets of lens mounts and in front of the motor and reflecting mirrors mount, each laser beam has a 102 degree field of view from the perpendicular to the base plate (see figure 10). Behind the motor and reflecting mirrors, the mount obstructs a fraction of each laser beam, limiting the field of view to 64 degrees from the perpendicular. Thus, the resulting field of view in the region in between the two beam axes is 166 degrees.

Along the same line, in the cone between the two sets of lens mounts the laser beam field of view perpendicular to the beacon base is 148 degrees (see figure 11). In this region, both laser beams are unobstructed.

In light of the limitations on the laser beacon's field of view, best results during flight tests will be attained if the beacon is mounted at a 45 degree angle to the hori-

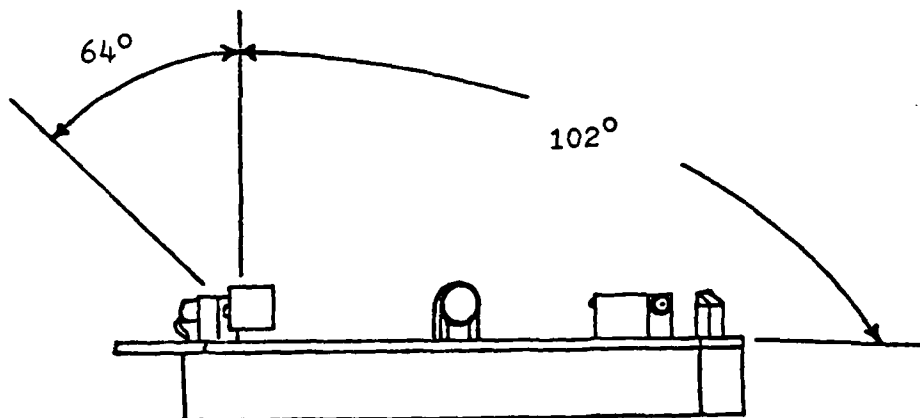


Figure 10: Beacon Orientation for a 166 Degree Field of View

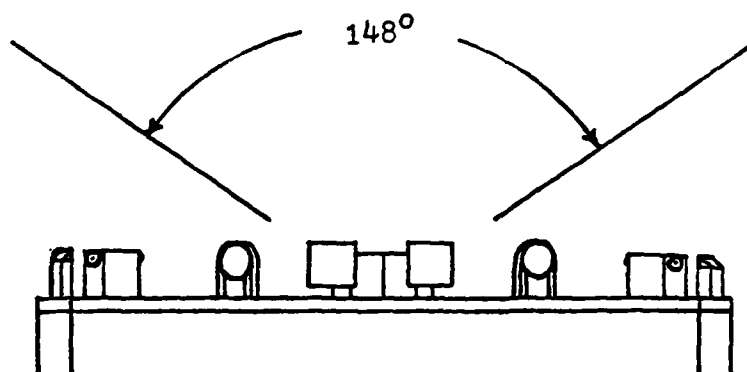


Figure 11: Beacon Orientation for a 148 Degree Field of View

zontal with the motor mount facing the tail section of the

helicopter and the area between the two mirror axes facing the forward section.

2.3.2 Rotation Accuracy Testing

The laser beacon, with the mirrors rotating at two revolutions per second, was also tested to determine the beam rotation accuracy. In this case, orthogonal laser beams swept past two detectors 30 meters downrange, and the time intervals resulting from the detected pulses were recorded. The detectors were placed 0.9 meters apart on a rotary table so that the incidence angle between the beacon and the perpendicular to the line joining the detectors could be varied. Twenty-five time interval measurements were recorded for each setting, and a mean, a standard deviation, and a percent error of the mean (standard deviation divided by the mean) were calculated.

Initial measurements resulted in unexpectedly large deviations with the error from the mean time interval above six percent. This error was traced to jitter caused by vibrations in the beacon reflecting mirror motor gearing, introducing an uncertainty in the time that the pulse from the photodiode in the detector was activated. It proved to be difficult to electronically filter out the jitter, since this type of jitter is pulse to pulse and many pulses are required in order to eliminate it. Eliminating the jitter would consequently slow the system response time to below an acceptable level.

Because it is essential to increase the rotation accuracy, the mirror motor was modified by placing a belt drive between the motor and the mirror. This reduced the jitter introduced by the gear train, and the error was reduced to less than 0.7 percent of the mean (see figure 12). The belt drive minimized the high frequency vibrations from within the beacon which had introduced the large errors in the measured time intervals. Initial tests of the rotation accuracy at a four revolution per second rate indicated that the error from the mean did not significantly differ from a two revolution per second rotation rate.

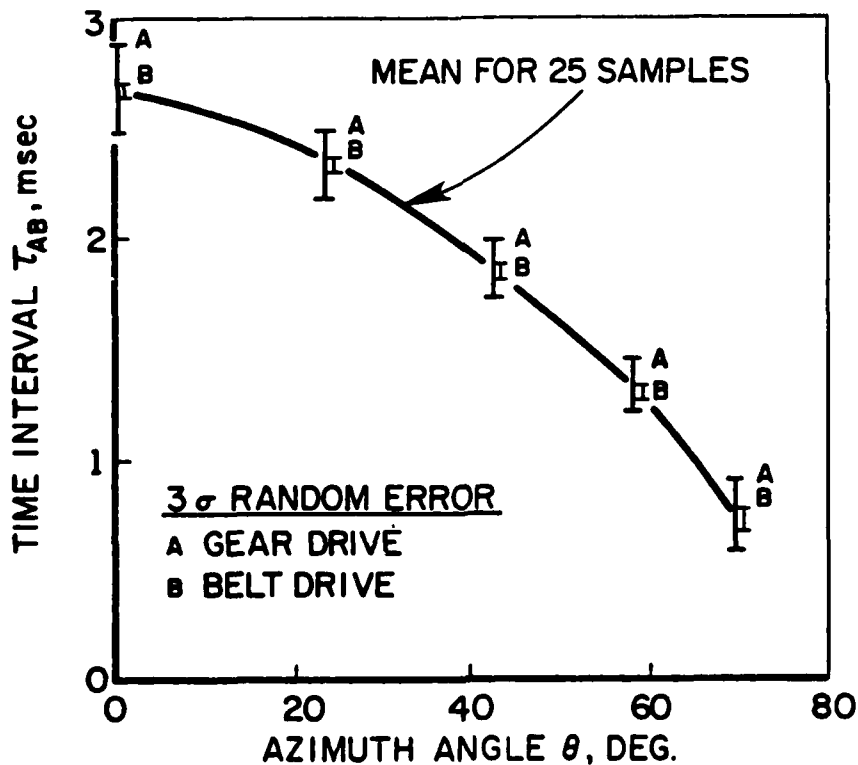


Figure 12: Mean Value and Error for Beacon Motor With and Without a Belt Drive

2.4 SUMMARY

Built specifically for flight on board a helicopter, the modified laser beacon possesses two lasers which emit light at a wavelength of 6328 Angstroms, and produces two orthogonal fan-shaped laser beams with approximately 166 degree fields of view. Each beam rotates at four revolutions per second and, without the glass plate, varies less than 0.7 percent from the mean.

The beacon is designed to have isolators to damp out helicopter vibrations above 16.64 Hz caused by compression forces and 12.42 Hz caused by shear forces. The calculated dynamic responses of the beacon structure do not match any of the expected excitation frequencies. In addition, the laser beacon will be mounted on the helicopter's nose at a 45 degree inclination angle to provide the best possible field of view.

Final testing of the laser beacon should include accuracy and field of view measurements with the glass plate in place. The beacon will undergo tests on a shaker table to assess the performance of the isolators. Finally, the laser beacon assembly will be utilized in both the field tests and the flight tests.

Chapter III

DETECTOR OPTICS

3.1 INTRODUCTION

The optical detector comprises a light collection and filtering optics apparatus which collects the incident light from the laser beacon. Due to the variety of flight positions to be assumed by the test aircraft, the detector must sense the laser beam from a wide field of view with simultaneous strong discrimination against background light from the sun and other sources. Since it is to be mounted on the tail of the YO-3A, the detector needs to be as lightweight and as aerodynamic as possible.

3.2 DETECTOR DESIGN

The optical detector design centers around three stages of light collection. First, the system collects the incident laser beam over a wide field of view. The light is then collimated and passed through a narrow pass-band optical filter to eliminate all but the desired light. Finally, the light is concentrated on a sensitive photodiode circuit. The output from the photodiode is amplified, filtered, and used to trigger a digital pulse for signal processing.

3.2.1 Spectral Filtering

The second stage of the optical system is concerned with filtering out all background light. This light rejection is achieved by using a narrow pass-band filter. Also called an interference filter, it passes a restricted range of wavelengths centered about a desired spectral region. For this project, the filter is centered about 6328 Angstroms, the laser's wavelength. All other light is filtered out. For example, a 30 Angstrom filter centered about the HeNe wavelength passes only 10^{-3} of the solar spectrum.

The narrow pass-band filter is interferometric in nature, since the transmission characteristics depend on the interference of light reflected from within the filter. It is constructed of multiple layers of material with different refractive indices. The thickness of each layer is dependent upon the desired wavelength, and the final light transmission through the filter depends on the interference of light reflected from the various layers. Thus, high transmission in the specific spectral region results while light, in both the short and long wave regions on either side of the pass band, is attenuated [3,4].

If light is incident upon the filter at angles other than perpendicular, the incoming light passes through the filter's layers at different spacing intervals. Consequently, the filter bandpass changes, which, in turn, severely limits the acceptance cone angle. This cone angle, ϕ , can be expressed by the equation [5]

$$\phi^2 = 2n_e^2(\Delta\lambda/\lambda)$$

where n_e is the effective refractive index of the interference filter and $\Delta\lambda/\lambda$ is the fractional bandwidth

For example, a ten Angstrom filter centered about the HeNe wavelength has an acceptance cone angle of only five degrees.

Consequently, the requirement for wide angle viewing with simultaneous spectral filtering implies that the light must be collimated before passing through the narrow pass-band filter. Otherwise, the desired incident light will be attenuated by the filter.

3.2.2 Detector Optics

In order to maintain a field of view approaching 180 degrees while utilizing an interference filter for spectral filtering, an optical system must collimate the laser light to within the filter's acceptance angle.

Perfect, or nearly perfect collimation, however, leads to a fundamental restriction on the optics due to the second law of thermodynamics. This law states that if light from a distributed source could be collimated, then it could be focused to a spot hotter than the original source. This means that light cannot be perfectly collimated unless it passes through an infinitely small point.

Since entropy is conserved in an ideal system, the following expression results [6]:

$$d \sin \theta = \text{constant}$$

where d is the collection aperture diameter and θ is the field of view cone half-angle, or the angle over which the light is to be collected

If the interference filter acceptance angle is ϕ , then the maximum ratio of the filter diameter, D , to the aperture diameter, d , for a collection angle of θ (a 2θ field of view) is

$$\frac{D}{d} = \frac{\sin \theta}{\sin \phi}$$

This same relationship can be applied when refocusing the light onto a photodiode after it passes through the filter.

A simple model for a wide angle collector (see figure 13) is a reflecting ball having an aperture diameter of $\sqrt{2} d$ in combination with a collimating lens whose diameter is D [7]. Light falling within the aperture diameter is reflected by the ball into the lens, where it is then collimated. Assuming a 180 degree field of view (θ is 90 degrees), the light's angular divergence ϕ' from the collimating lens is

$$\sin \phi' = \frac{d/2}{\sqrt{f^2 + (d/2)^2}} \approx \frac{d/2}{f}$$

where f is the focal length of the lens

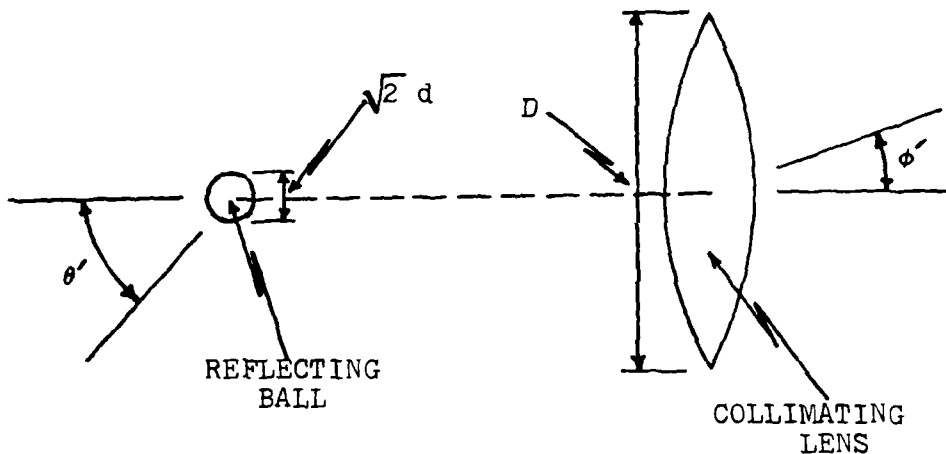


Figure 13: Model of a Wide Angle Collector Consisting of a Reflecting Ball and a Collimating Lens

The thermodynamic limit for this optical system occurs when the focal length is equal to $D/2$. This optimum can be reached only with reflective optics, since the ideal collection f number is one-half, and, in practice, the lenses with the shortest focal numbers (except for fresnel lenses) have f numbers approaching only one. This corresponds to having lenses with focal lengths equaling their respective diameters. Consequently, these lenses cannot approach the thermodynamic limit. In addition, because light collection is proportional to the inverse of the f number squared, as a

result, the $f = D$ lenses collect only one-quarter of the theoretically available light from the $f = D/2$ lenses. Also, additional losses in light collection occur due to reflections from the lens surfaces.

3.2.3 CPC Design

With conventional optics limited to an f number of one due to thermodynamic considerations, a more efficient collection system is desired. R. Winston and his colleagues have developed a compound parabolic concentrator (CPC). Designed to isentropically focus light, this collector has been found to approximate closely the thermodynamic limit with an f number approaching one-half. It is nonimaging and is of considerable interest for solar energy collection [7,8].

The CPC is basically a parabolic reflector with the tip cut off and the sides brought close together. Solar collection is achieved by aiming the wide end at the sun and collecting the light at the focus. However, if the CPC is turned around, light from a wide field of view can be "collimated"--that is, light exits the CPC at a cone angle which is less than the entrance cone angle.

The detectors used to collect the laser beam from the beacon incorporate the compound parabolic concentrator as the basis for the optical system (see figure 14). Each detector consists of two CPC's, a narrow pass-band filter, and

a photodiode. Light incident at wide angles passes through the small aperture diameter of the first CPC and is "collimated". After passing through the filter, the light is refocused by the second CPC where a photodiode, placed at the tip of the CPC, detects the laser beam.

The input end of the detector, or the first CPC, is cut in such a manner that the incoming light passes through an entrance aperture diameter, d , with up to a 90 degree acceptance angle θ (corresponding to a 180 degree field of view). The CPC's exit aperture angle, ϕ , is selected by the limit of the interference filter. The aperture angle is smaller than the filter's cone acceptance angle, ϕ , so that all the laser light is "collimated" enough to pass through the filter.

For a 180 degree field of view, the required diameter for the entrance aperture can be found by the relation

$$d = D \sin \phi$$

where D is the filter's diameter

The geometrical definition (see figure 15, which is referenced from [8]) for the compound parabolic concentrator is a surface of revolution about the z -axis constrained by the following expressions [8]

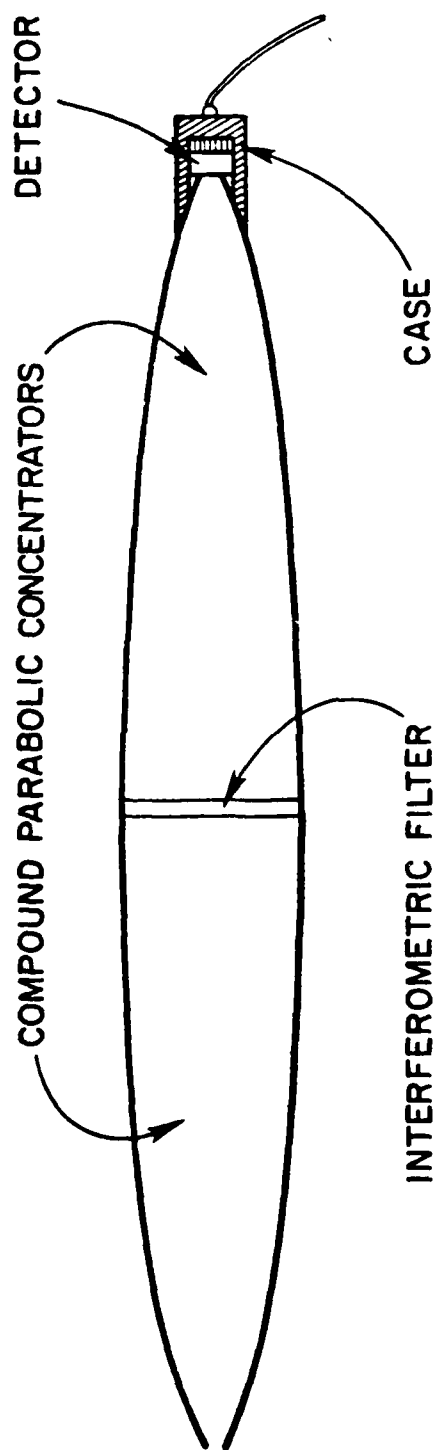


Figure 14: CPC Detector Design, Consisting of Two CPCs and an Interference Filter

$$r = \frac{2\bar{f} \sin(\eta - \phi)}{1 - \cos \eta} - \frac{d}{2}$$

$$z = \frac{2\bar{f} \cos(\eta - \phi)}{1 - \cos \eta}$$

$$L = \frac{(D + d)}{2} \cot \phi$$

where

$$\bar{f} = \frac{d}{2}(1 + \sin \phi)$$

The angle η is a variable defined such that, at $z = 0$, it is equal to 90 degrees plus the exit divergence angle, ϕ . As z increases, η decreases, and, when z equals the desired length, L ,

$$\eta = \tan^{-1} \frac{(D + d)}{2L}$$

Figure 15 shows how η is defined.

creases. The CPC length increases as the exit aperture diameter, D , increases. In addition, the CPC length decreases with an increasing exit divergence angle, Φ , and there is a dramatic rise in the length of the CPC if Φ is desired to be less than ten degrees.

Of course, increasing the exit divergence angle affects both the exit and the entrance aperture diameters in one of three ways. Increasing Φ increases the entrance aperture diameter, d , with the exit aperture diameter, D , held constant. Conversely, if the entrance aperture diameter is not allowed to change, the exit aperture diameter decreases with an increasing Φ . Finally, the exit aperture diameter decreases while the entrance aperture diameter increases in a ratio corresponding to the sine of the exit divergence angle.

These interrelationships must be considered when designing a CPC detector for a specific use. If size is a critical factor, tradeoffs exist between the CPC length and both the field of view and the exit divergence angle. For example, if it is desired that the CPC be as small as possible, a penalty in the exit divergence angle is incurred (but with small variations in the desired field of view). Increasing the angle Φ not only affects the two aperture diameters, but it also decreases the effectiveness of the spectral filtering. For this research project, the CPC was designed to acquire a 180 degree field of view with a small exit divergence angle and a fixed exit aperture diameter.

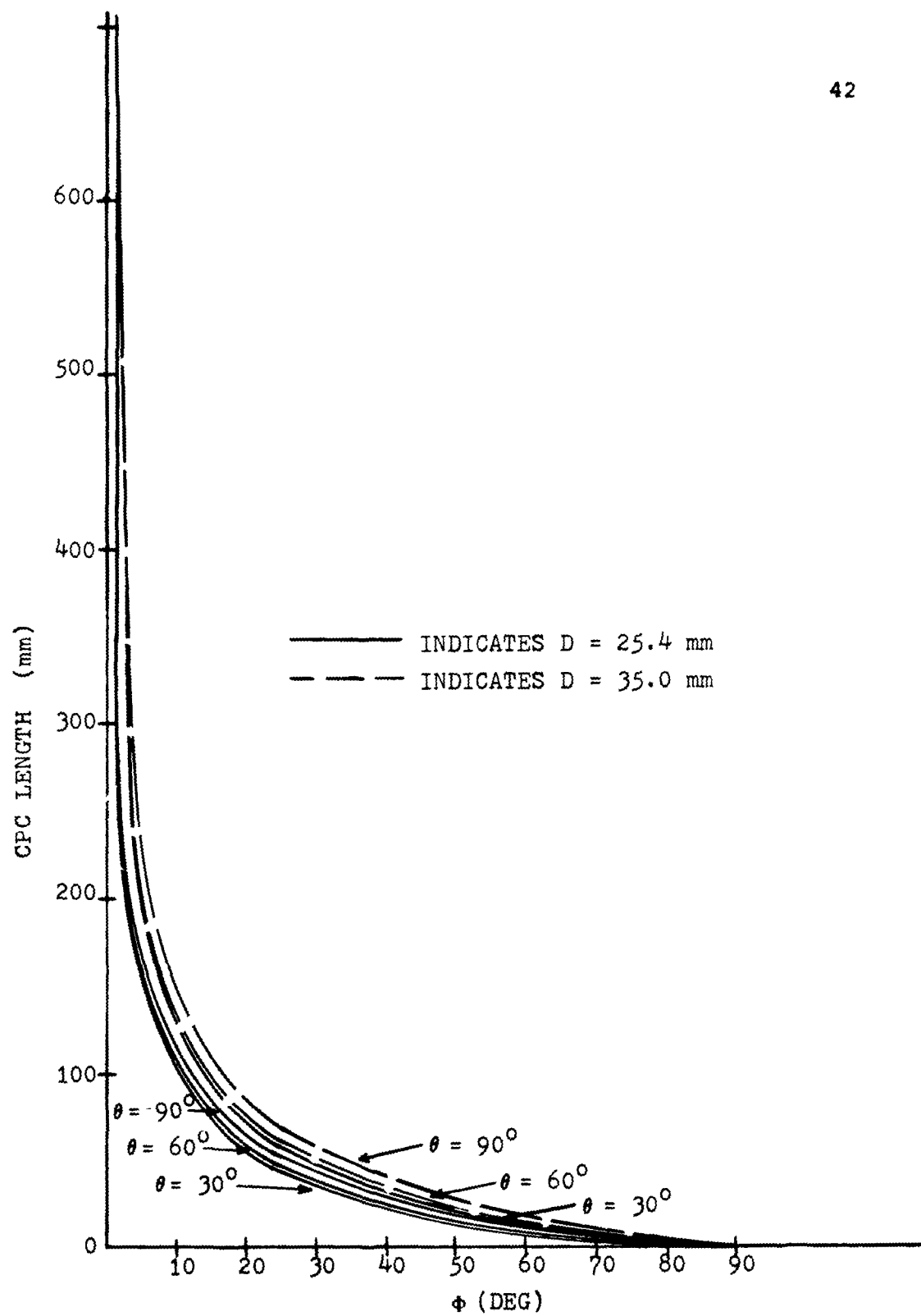


Figure 16: CPC Length Versus Exit Divergence Angle for Varying Fields of View and Varying Exit Aperture Diameters

The second CPC is constructed in an identical manner to the first one, thus insuring maximum collection efficiency.

Initial dimensions were calculated for a 180 degree field of view compound parabolic concentrator with an exit divergence angle, Φ , of 5.3 degrees and an exit aperture diameter of 20.1 mm (the diameter of both the ten Angstrom filter and the thirty Angstrom filter used in the experiments). The entrance aperture diameter was required to be 1.85 mm, and the overall CPC length was 118.31 mm. The CPC's actually used had somewhat different dimensions, as discussed below.

3.3 TESTING AND MODIFICATIONS

The optical system is designed to provide the maximum collection efficiency possible while avoiding losses due to interactions brought about by conventional lensing systems optical surfaces. In order to compare a lensing system with the CPC detector, prototypes of the two were constructed.

3.3.1 Lens System

The lens collector system constructed (see figure 17) is composed of a wide-angle (190 degree) fisheye lens placed at the focus of an f 1 plano-convex lens. An interference filter follows, as well as a second f 1 plano-convex lens, with a silicon photodiode placed at its focus. Light from wide angles enters the fisheye lens and is collimated by the first plano-convex lens. The light then passes through the

filter, and the second plano-convex lens focuses it on the detector. Tests showed this lens system to have a field of view approaching only 86 degrees (a 43 degree incidence angle). This small field of view is not acceptable for the detector requirements, since it is desirable for the field of view to approach 180 degrees. Several problems with this collector were observed during testing. Calculations for an $f/1$ lens system with a 3.18 mm aperture opening, a 25.4 mm filter diameter, and a filter acceptance angle of five degrees showed that the angular acceptance was only 44.2 degrees. In addition, optical vignetting, as well as reflections from the lenses, degraded the collection efficiency. Consequently, rather than attempting to optimize the lens collector system, the focus on designing a detector was switched to the CPC detector system.

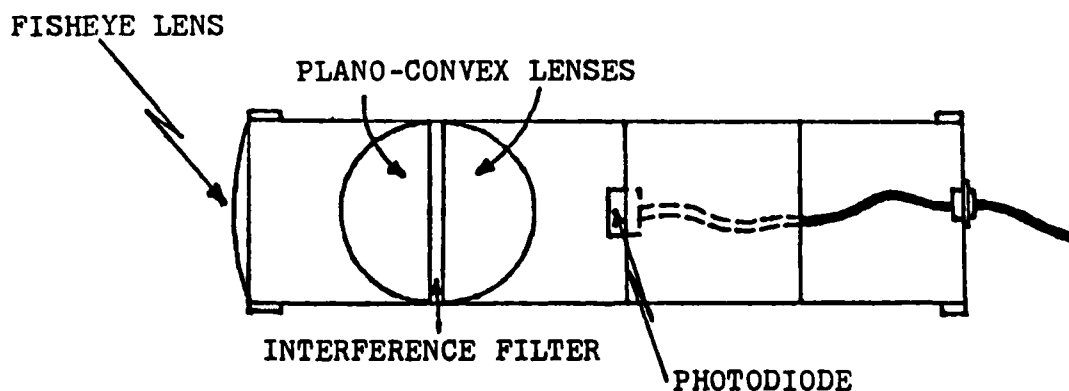


Figure 17: $F/1$ Lens Collector System Consisting of Two Plano-Convex Lenses and an Interference Filter

3.3.2 CPC Detector System

Tests were also conducted with the CPC detector. In order to quantify the detector's performance over a wide field of view, the photodiode voltage output was measured under varying conditions.

Due to the expense involved in constructing a CPC to meet original design specifications, the CPC's used were made from a mandril previously designed and constructed by personnel at the University of Chicago. Each compound parabolic concentrator utilized for the experiments had an entrance aperture diameter of 2.25 mm, an exit aperture diameter of 18.0 mm, and a length of 80.36 mm. The exit divergence angle for each detector was 7.18 degrees. The assembled CPC detector weighed less than one kilogram, had a maximum diameter of 34.93 mm, and was 163.90 mm long.

The detector was mounted on a rotary base such that at a zero incidence angle the entrance aperture was aimed directly at the laser beacon and maximum voltage was recorded by the photodiode. As the base rotated, the detector efficiency as a function of incidence angle was recorded. The effects of noise on the detector efficiency measurements were minimized with the use of a lock-in amplifier system tuned to the particular frequency of a chopping wheel placed in front of the laser beam.

Initial tests conducted without any filters in the detector uncovered a substantial blind spot at incidence angles

between five and ten degrees (see figure 18). The blind spot occurs because in this region of incidence angles, light exits the second CPC at angles approaching 90 degrees. Consequently, the light encounters the silicon photodiode at grazing incidences, and substantial reflectivity from the photodiode results. This difficulty was alleviated by cutting a bit off the tip of the second CPC and opening the exit aperture by approximately 33 percent to 3.05 mm. Thus, instead of a 90 degree exit divergence angle, the opening reduced this angle to 49 degrees, and the blind spot was effectively eliminated.

Tests of both the original and the modified detectors showed a large peak in the intensity at angles less than five degrees due to the direct incidence of the laser beacon on the photodiode. At larger incidence angles, the intensity uniformly decreased as the incidence angle increased.

The next set of tests were conducted with a ten Angstrom narrow pass-band filter inserted between the two compound parabolic concentrators. A blind spot was again observed (see figure 19) at small incidence angles due to the fact that the maximum filter acceptance angle (a five degree angle) is less than the maximum angle of light exiting the first CPC (a seven degree angle). Light encountering the filter in the region surrounding these critical angles was attenuated.

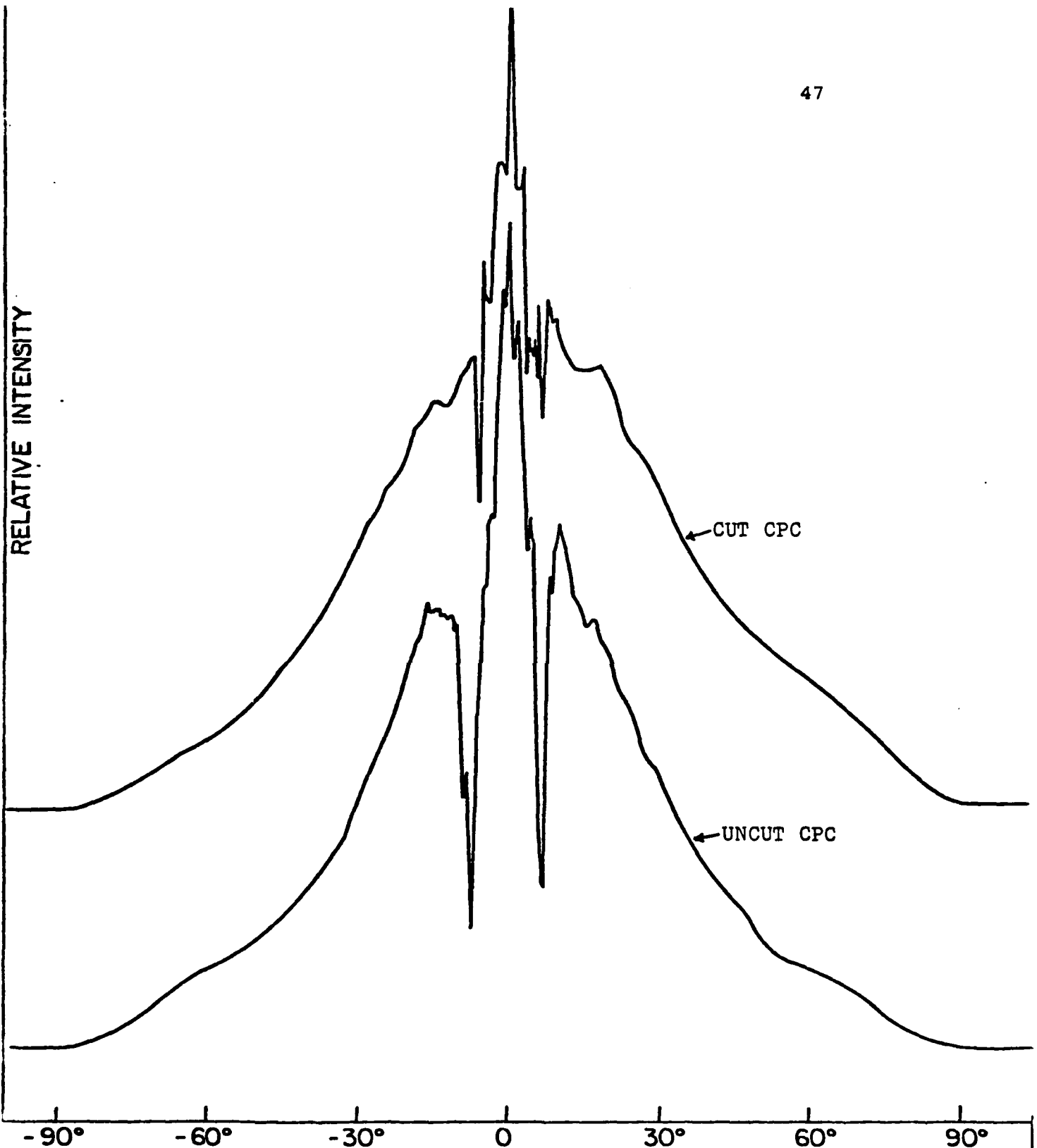


Figure 18: Intensity Versus Incidence Angle Without Interference Filters for Both a Standard CPC and a CPC With a Bit Cut Off

The ten Angstrom filter was replaced by a 30 Angstrom filter, and the tests were repeated (see figure 19). With the larger bandwidth filter the blind spot was alleviated. The tests with both filters showed that the intensity of the collected light decreased as the width of the narrow pass-band filter decreased. Due to the constant noise threshold, the result was a decreased field of view for the detector.

Both filters discriminated against sunlight when both the sun and the laser were in the detector's central field of view. The detectors sensed the laser beams, though with a decreased signal to noise ratio, even when the laser beacon was near the edge of the detector's field of view and the sun was in the center of the field of view. Thus, with the narrow pass-band filters, the CPC detector successfully observed the laser beacon in the presence of background sunlight. Tests were conducted to quantify this observation. The CPC detector with the 30 Angstrom filter was mounted on the rotary base and a high intensity lamp was placed at a 45 degree angle relative to the laser beacon. The lamp modeled the sun and was adjusted so that at an incidence angle of 45 degrees, the detector was facing the lamp directly. The photodiode's voltage output was recorded as the incidence angle varied both with and without the pseudo sun. The signal to noise ratio decreased in the presence of the model "sun," but the output pulses were still detectable and the field of view was not significantly reduced. With the lamp

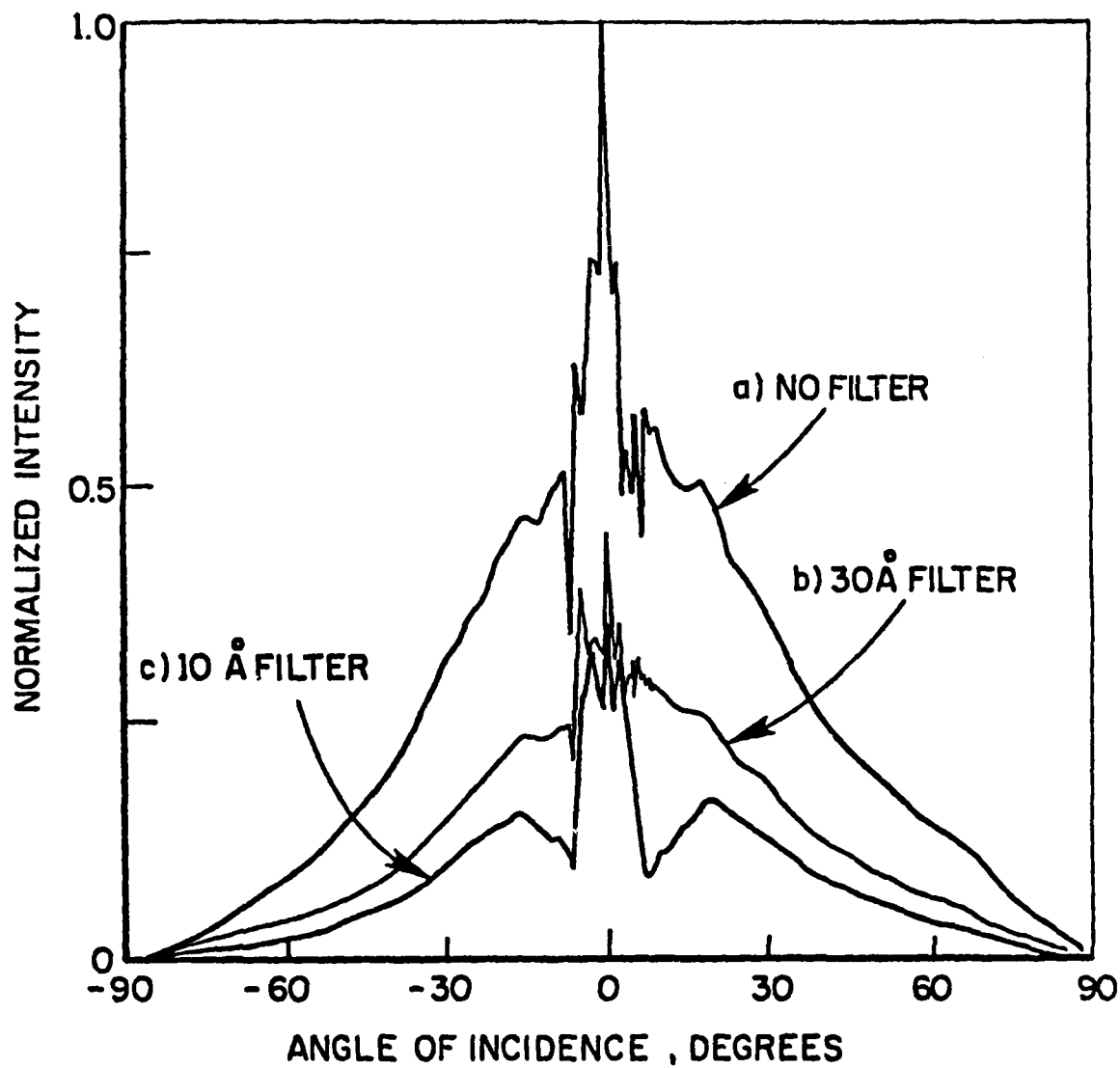


Figure 19: Normalized Intensity With a) No Interference Filter, b) a 10 Angstrom Filter, and c) a 30 Angstrom Filter

turned on, the field of view was determined to be 158 degrees, whereas it was 170 degrees without "sunlight." Similar results were obtained when the 30 Angstrom filter was replaced with the ten Angstrom filter. The field of view in the presence of the sunlight, however, was reduced to 130 degrees. With no pseudo sun it was approximately 140 degrees. The field of view decreased with the ten Angstrom filter in the detector because, as is shown in figure 19, the ten Angstrom filter passes less light than the 30 Angstrom filter.

Field of view measurements were also conducted in direct sunlight. The laser beacon was set up approximately 30 meters from two detectors. The detectors, with the 30 Angstrom filters placed inside, were positioned 0.9 meters apart on the rotary table, and the time intervals between each detector sensing the laser beam sweeps were recorded as the table rotated. The maximum field of view measured was 168 degrees, but after a 75 degree incidence angle (a 150 degree field of view), noise crept into the measurements so that the detectors began missing pulses. This field of view (150 degrees) was found to be less than that measured during the experiments with the pseudo sun (158 degrees) because, in these experiments, the sun produced a higher intensity noise content than the high intensity lamp. Consequently, an accurate field of view for the CPC detector in direct sunlight is limited to approximately 150 degrees.

3.4 SUMMARY

The detector system to be used for this research project is the compound parabolic concentrator detector. Effectively discriminating against background light from the sun and other sources, it senses, with a field of view approaching 150 degrees, beams emanating from the laser beacon. With the 30 Angstrom filter in place, the overall length of the CPC detector is 163.90 mm (excluding the photodiode and preamplifier assembly) and the maximum diameter is 34.93 mm. Each detector weighs less than one kilogram. The small size and light weight of each detector is advantageous since the detector array will be placed on the tail of the YO-3A.

Chapter IV

DETECTOR ELECTRONICS

4.1 INTRODUCTION

The electronics package passes the photodiode pulse to the microprocessor system for signal interpreting. The purpose of the package is to process the raw photodiode signal to compensate for background interference, especially low frequency solar background. Utilizing frequency filtering networks to pass the pulse, the electronics are designed for low noise and high gain, and are compatible with the microprocessor. Since the electronics package is to be mounted in the target plane--the YO-3A--it must be as compact as possible and operate off the aircraft's 28 volt DC power supply.

4.2 PACKAGE DESIGN

4.2.1 Electronic Filters

Essential to the electronics design is the inclusion of filters that eliminate interference. The band-pass filter rejects the low frequencies of the sunlight's temporal spectrum, yet passes most of the laser beam's energy. In

addition, the filter rejects light reflections whose temporal characteristics are different from those of the laser beams. It rejects the high frequency white noise, shields the electronics system from background noise, and filters out feedback from the high gain output.

The characteristics of the band-pass filter are determined by calculating the expected pulse frequency range. Assuming that the beacon beam width is larger than the detector entrance aperture and that the laser beam is focused at the range to be considered, the pulse on time measured between the $1/e^2$ intensity points is

$$\Delta t = \frac{w(R)}{R} \frac{\Delta r}{2\pi}$$

where $w(R)$ is the laser beacon width, R is the range from the beacon to the detector array, and Δr is the elapsed time between the beam sweeps

If the laser beam signal is such that the $1/e$ intensity point occurs at $\Delta t/2$, the pulse intensity, h , as a function of time, can be modeled as

$$h(t) = e^{-2t^2/(\Delta t/2)^2}$$

Defining Δf to be the bandwidth to the one-half power point (the 3 dB point), the Fourier Transform, H , of the pulse is then (by the similarity theorem) [9]

$$H(f) = \frac{\pi \Delta t^2}{8} e^{-(\pi^2 \Delta t^2 f^2)/8}$$

where

$$\Delta f = \frac{\sqrt{8}}{\pi \Delta t} \ln 2$$

and f is the pulse frequency

Thus, a gaussian time pulse with a width Δt of ten microseconds has a frequency distribution with a width Δf equal to 62 KHz (see figure 20). The electronic filter excludes the DC voltage and acts as a band-pass to eliminate both the low frequency and the high frequency noise [10].

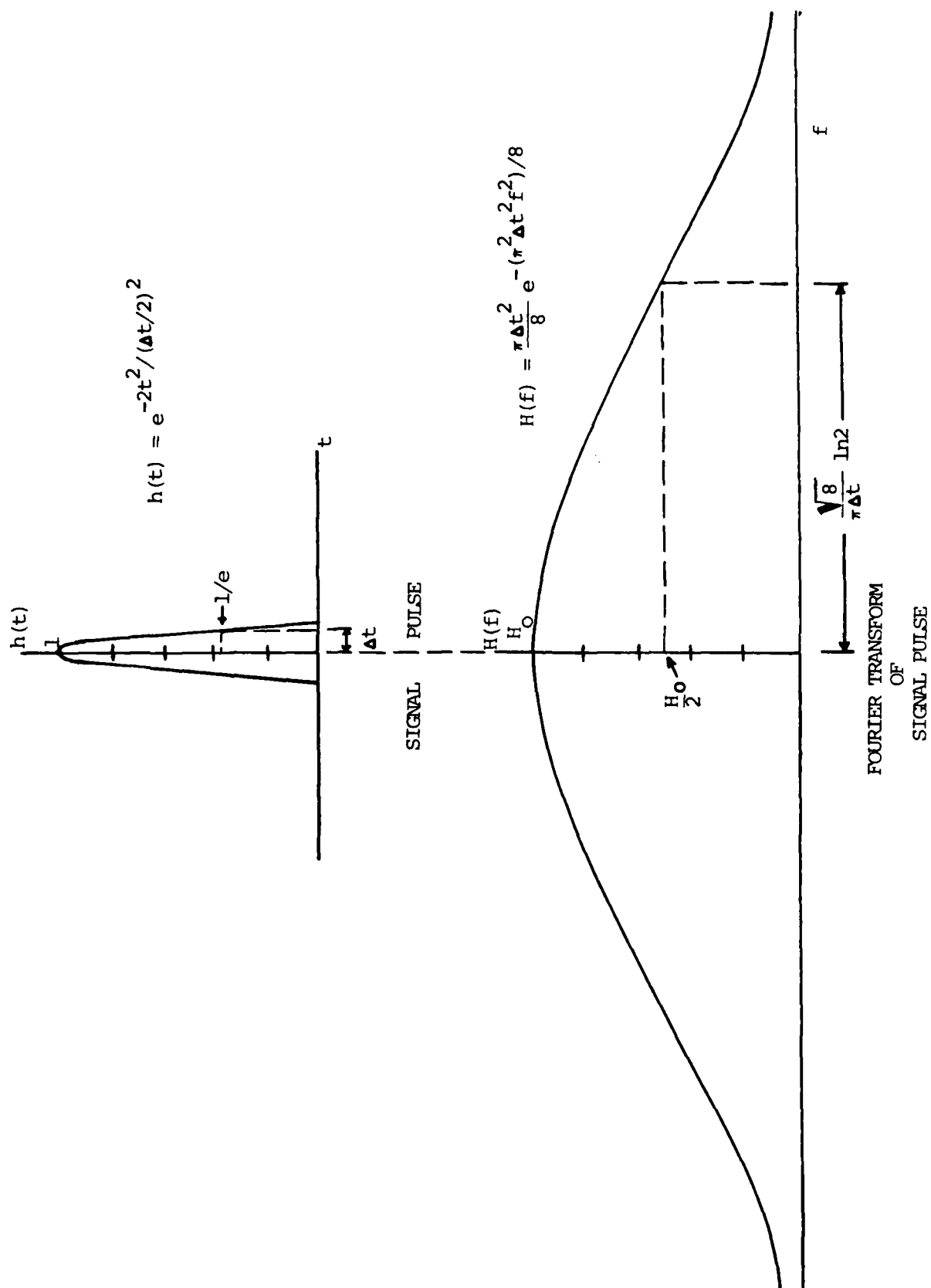


Figure 20: Gaussian Laser Beam Signal and its Fourier Transform

4.2.2 Threshold and Gain Adjustment

A five volt digital pulse is the output to be passed to the microprocessor unit for signal processing and signal computation. As shown in figure 21, the pulse passes through various stages as it is processed from the raw photodiode signal to the final digital pulse form.

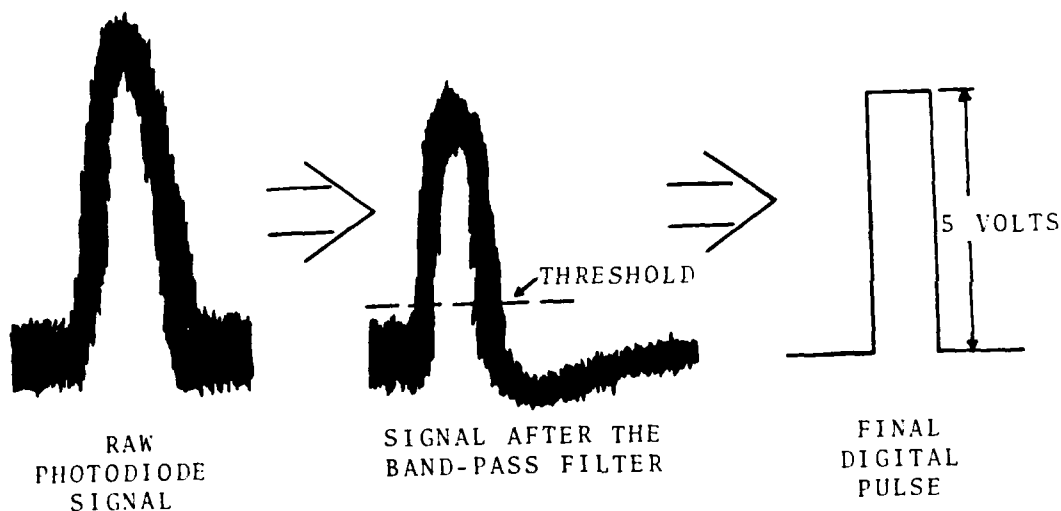


Figure 21: Stages of the Electronic Pulse as it is Processed From a Raw Photodiode Signal to the Final Digital Pulse Form

A threshold is needed to trigger this digital output and must be variable in order to accommodate changes in the background light and signal strength. Background light depends upon the detector's position with respect to the sun and other light sources. The signal strength is dependent

upon the relative position between the laser beacon and the detector and decreases with increasing range and deviations off the zero incidence angle. The threshold level is to be set either manually or by logic in the microprocessor.

High gain output from the photodiode is required to insure accurate discrimination between the signal and background noise. The field of view is limited by the amount of gain available. However, the gain cannot be too high, or the amplifier will saturate. In addition, the pulse from each detector must be nearly identical in order to reduce inherent errors in the trigger time interval. An adjustable gain is designed to pass the maximum signal possible, while keeping the pulse magnitudes from each of the detectors uniform.

4.2.3 Electronic Components

The electronics system (see the schematics in figures 22, 23, and 24) incorporates all four detectors in the array and is installed on board the YO-3A. Threshold and gain adjustments are accessible while the system is packaged in the aircraft. Light emitting diodes for each detector are triggered every time a laser beam is sensed, which allows the engineer on board the YO-3A to insure that the electronics system is functioning properly. A six pole high band-pass filter is included to eliminate low frequency noise below 250 Hz (see figure 25). This feature is valuable in the

bench test phase of the project when undesirable 60 and 120 Hz noise is introduced by lights and other sources. In addition, low frequency noise elimination is especially desirable during the flight tests for several reasons. Not only do aircraft generate noise primarily in the region of low frequencies, but the sun also has large low frequency noise components. Finally, low frequency noise can be caused by atmospheric scintillation, clouds, and other phenomena.

Meret MDA 530-680 silicon photodiodes are utilized to detect the laser beams. With a relative spectral responsivity suited to the project requirements, each photodiode includes a built-in amplifier. The amplifier's proximity to the photodiode eliminates problems with signal attenuation and noise introduced by long leads connecting the two electronic components. Moreover, since packaging an amplifier next to the detector leads to size and aerodynamic constraints, the photodiode utilized is more efficient. The protective cover on the photocell is removed to allow the cell to be as close to the CPC exit aperture as possible. This is important since the light is focused at the exit aperture, and a tremendous amount of light is lost if the photocell is separated from the end of the CPC.

A high gain first stage and the associated preliminary electronics are packaged next to the photodiode, increasing the signal output and eliminating noise from pickup in any leads. The remainder of the electronics is packaged on board the YO-3A's equipment compartment.

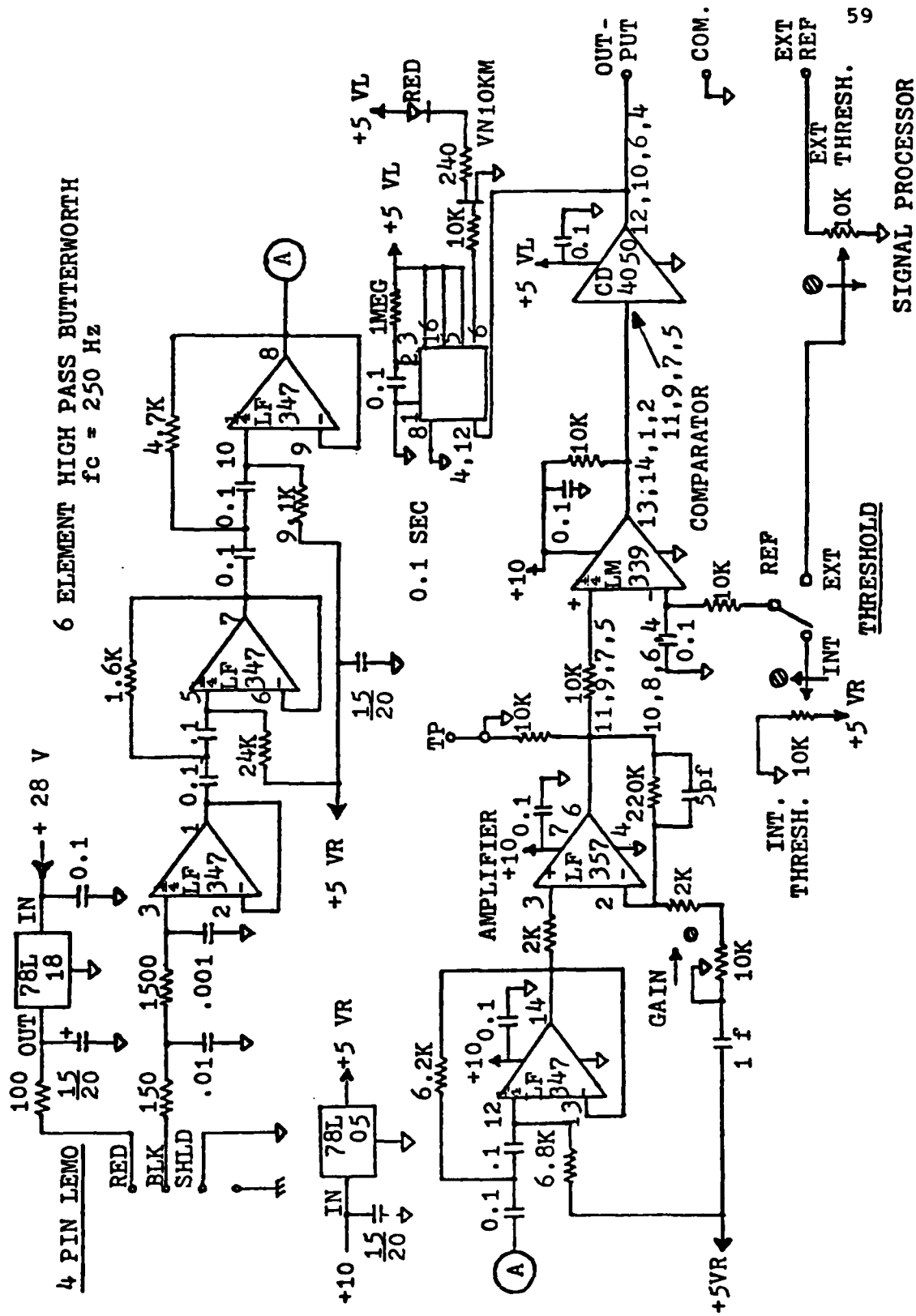


Figure 22: Schematic of the Electronics System

Figure 24: Schematic of the Sensor and the Preamplifier

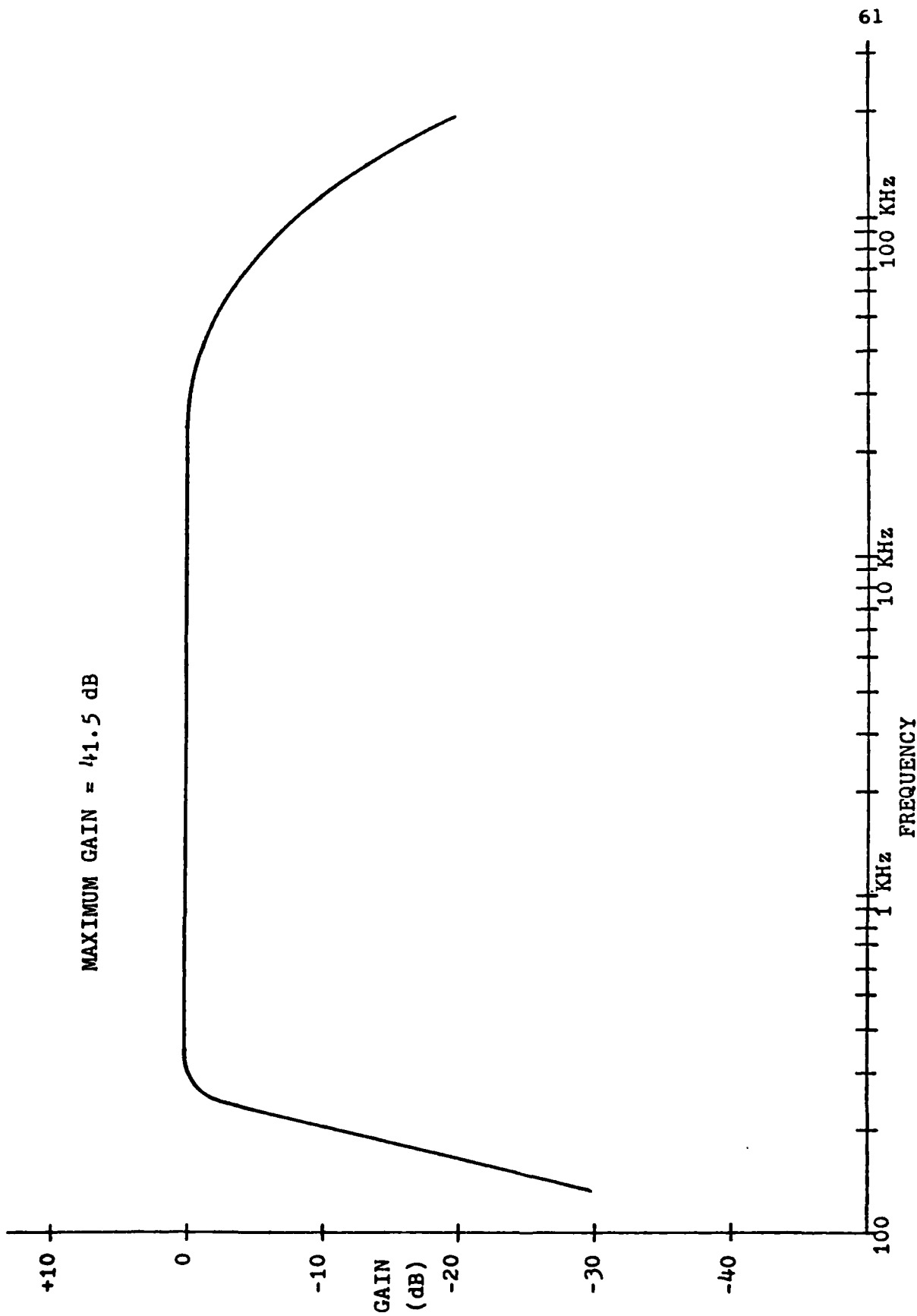


Figure 25: Bode Plot of the Measured Response of the Electronics System

4.3 SUMMARY

Two iterations of the electronics package were constructed as prototypes for the four-detector electronics system. The first was designed for processing the signals from a single detector while the second prototype accommodated two detectors. The refined electronics package incorporates modifications from the first two prototypes and is built specifically for installation in the YO-3A. Each photodiode and preamplifier assembly is small and lightweight, which is advantageous since they are to be connected to the CPC detectors on the tail of the YO-3A.

The filter rejects high frequency shot noise and low frequency noise below 250 Hz. Consequently, the electronics package passes the incident laser beam's energy while rejecting most of the background interference. The threshold can be changed to pass only the desired pulse. The adjustable gain allows each pulse to be as identical as possible to reduce trigger errors.

Chapter V

DETECTOR ARRAY

5.1 INTRODUCTION

As stated previously, the objective of this research project is to achieve both high range accuracy and precise measurements of azimuth and elevation between the YO-3A and the helicopter. An array of detectors is used to yield the required position information in terms of time intervals between pulses from adjacent detectors. In order to calculate a two-dimensional position measurement of the range and azimuth between the two aircraft, three detectors are required to interpret pulses from a single lateral beacon sweep. However, for a three-dimensional position measurement involving range, azimuth, and elevation, four detectors are required. These detectors intercept both vertical and lateral sweeps of fan-shaped laser beams. In order to provide accurate position information, the array configuration is critical.

5.2 TWO-DIMENSIONAL POSITION CALCULATION

For two-dimensional location measurements with three detectors, it is convenient for the detectors to be arrayed in a right isosceles triangular configuration. If the separation distance between the detectors and the laser beacon is large in comparison with the detector separation, then it can be assumed that the focused laser beam is a parallel line sweeping past the detectors. As the line intersects each detector, an electronic pulse is produced.

Referring to figure 26, the measured time intervals between the detectors are τ_{AB} and τ_{BC} . With a beacon sweep speed, v , being calculated with respect to the distance between the detectors and the beacon axis (R), the speed is

$$v = 2\pi R / \Delta\tau$$

where $\Delta\tau$ is the period of rotation

At a given speed, v , the measured time intervals correspond to the projected distances between the detectors (as seen from the beacon) such that

$$d'_{AB} = v \tau_{AB}$$

$$d'_{AB} = v \tau_{AB}$$

Since the detectors, as configured, form equal legs of a right triangle, the following results

$$d_{AB} = d_{BC} = \sqrt{(d'_{AB})^2 + (d'_{BC})^2}$$

From geometrical considerations, the calculated range, R , is then

$$R = \frac{d_{AB}}{2\pi N \sqrt{\tau_{AB}^2 + \tau_{AB}^2}}$$

The azimuth angle, ψ , is the angle from the line connecting the two detectors and the beacon axis, and can be found by the relationship

$$\psi = \tan^{-1}(d_{AB}/d_{BC}) = \tan^{-1}(\tau_{AB}/\tau_{BC})$$

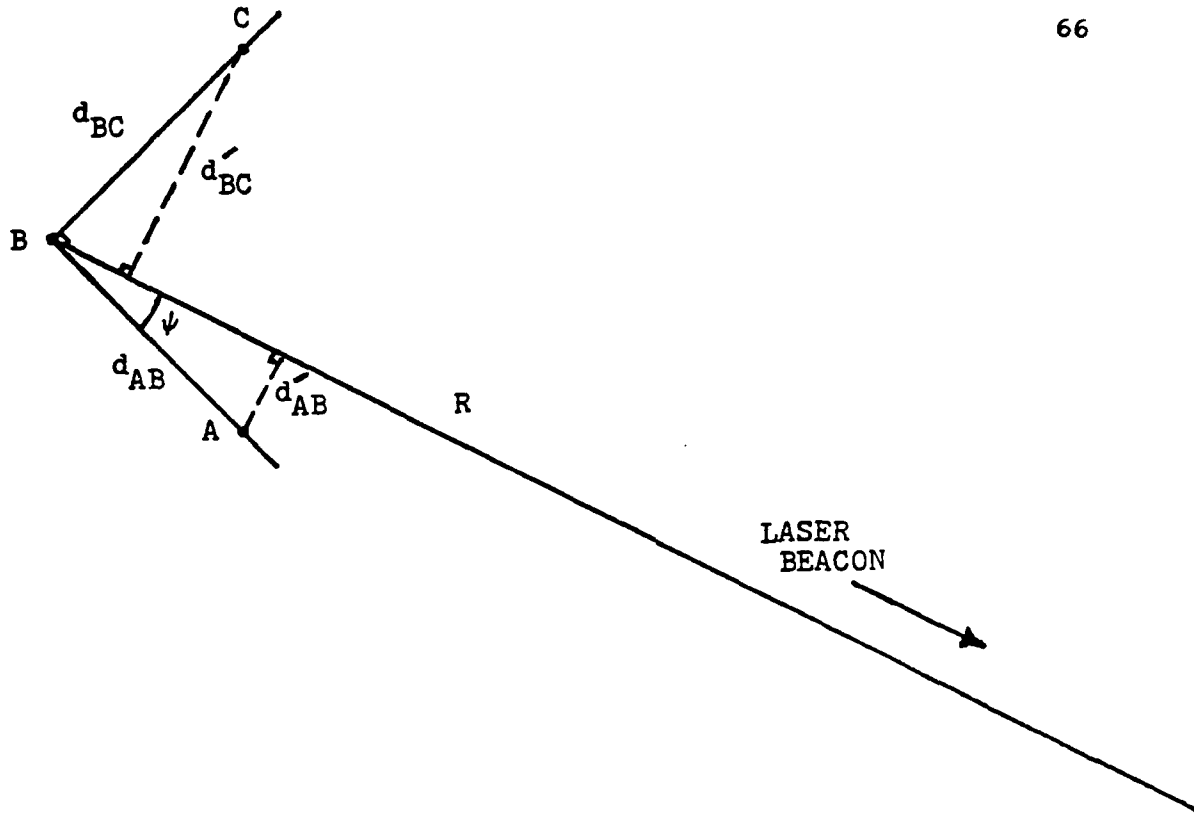


Figure 26: Two-Dimensional Geometry for Relative Position Calculations

5.3 THREE-DIMENSIONAL POSITION CALCULATION

The calculations for the three-dimensional location measurements are similar to those made for the two-dimensional case. However, the addition of another dimension requires not only a second laser beam orthogonal to the first, but also a fourth detector in the array. In the new configuration, all detectors are mutually perpendicular to each other, as shown in figure 27. Derivation of the following trigonometric relations was accomplished by Professor Sweet and E. Y. Wong, a graduate research assistant at Princeton University.

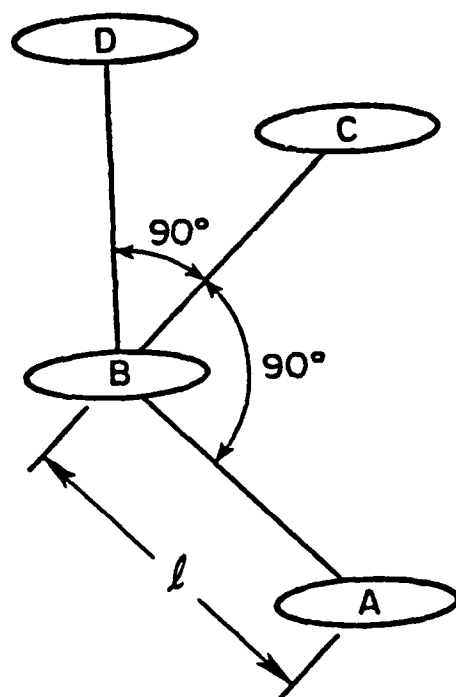


Figure 27: A Four Detector Array

If the time intervals are clocked from a common trigger, the interval between pulses 'i' and 'j' for a lateral sweep is

$$\tau_{ij} = \tau_j - \tau_i$$

For a vertical sweep the time interval is

$$v_{ij} = v_j - v_i$$

For $\nu_{BC} > \nu_{BA}$, and a beacon sweep period of $\Delta\tau$, the following relationships result for the range R , azimuth ψ , and elevation β (figure 28).

$$R = \frac{\Delta\tau}{2\pi} \sqrt{\frac{1}{\tau_{AB}^2 + \tau_{BC}^2} + \left(\frac{\nu'_{BC}}{\nu_{DB}^2 + \nu_{BC}^2} \right)^2}$$

$$\beta = \tan^{-1}(\tau_{AB}/\tau_{BC})$$

$$\psi = \tan^{-1} \left[\frac{\nu_{DB}^2 + \nu_{BC}^2}{\nu'_{BC} \sqrt{\tau_{DB}^2 + \tau_{BC}^2}} \right]$$

where

$$\nu'_{DB} = \nu_{DB}$$

$$\nu'_{BC} = \nu_{BC} \sqrt{\nu_{BC}^2 + \nu_{BA}^2} / |\nu_{BC}|$$

If ν_{BC} is less than ν_{BA} , ν_{BA} is substituted in the above equations for ν_{BC} while ν'_{BA} is substituted for ν'_{BC} . These equations are invariant to changes in the laser beacon orientation in the pitch and yaw directions, if it is assumed that the detector array and beacon vertical axes have a zero relative roll angle. The array can change its yaw and pitch orientation relative to the YO-3A, as long as

these changes are accounted for with respect to the aircraft coordinate system.

However, since the above equations assume that the detector array and the laser beacon vertical axes are parallel, the equations no longer hold if a relative roll angle exists between the two axes. Consequently, the existence of a roll angle implies that a coordinate transformation must be introduced in order to change the axis orientation back to one with a zero relative roll angle.

As can be seen in figure 29, the lateral beacon sweep encounters detectors B and D at the same instant in time when the vertical axes are parallel. If, on the other hand, a roll angle is introduced, the beam hits one detector before the other. The time interval between detectors B and D in a lateral beacon sweep is τ_{BD} . As in the two-dimensional case, the apparent distance (as seen by the laser beacon) between the two detectors is

$$d'_{BD} = v \tau_{BD}$$

Thus, the relative roll angle, ϕ , between the two vertical axes can be calculated.

$$\phi = \sin^{-1} \frac{d'_{DB}}{d_{DB}}$$

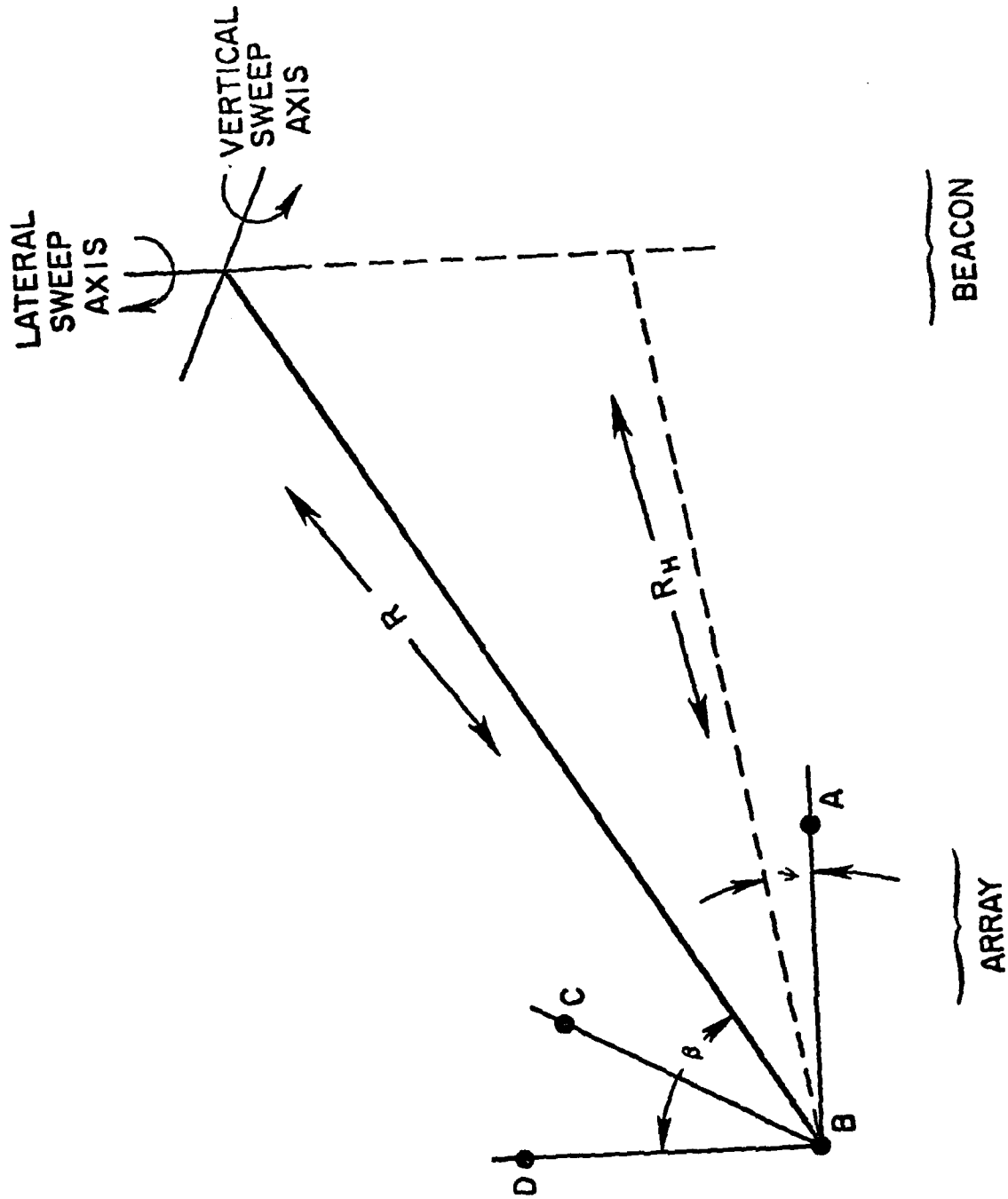


Figure 28: Three-Dimensional Geometry for Relative Position Calculations

An Euler angle coordinate transformation [11] can be performed so that the three-dimensional position equations are again valid.

$$\begin{bmatrix} x \\ y \\ z \end{bmatrix} = \begin{bmatrix} 1 & 0 & 0 \\ 0 & \cos\phi & -\sin\phi \\ 0 & \sin\phi & \cos\phi \end{bmatrix} \begin{bmatrix} x \\ y \\ z' \end{bmatrix}$$

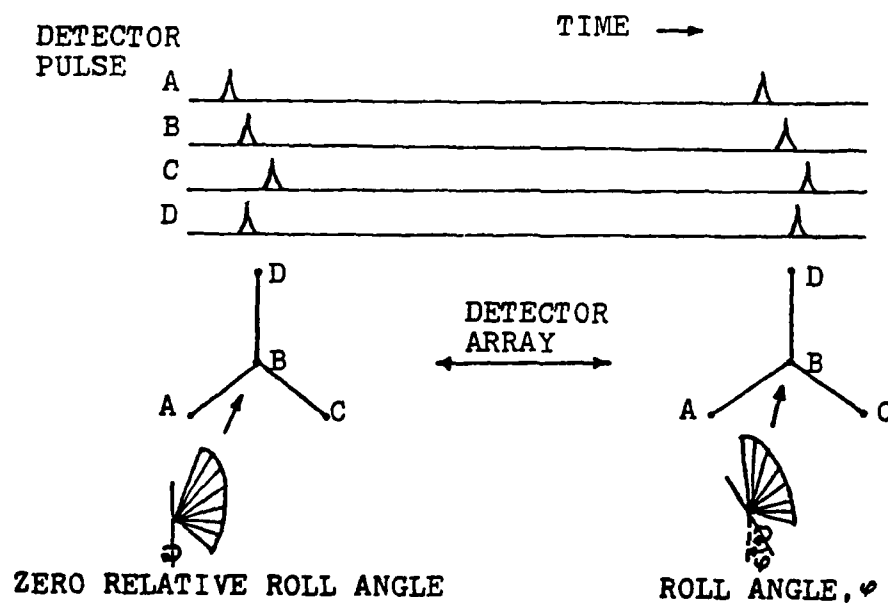


Figure 29: Lateral Beacon Sweeps With and Without a Roll Angle

The position determination equations actually utilized for this research project were developed by G. Russell, a graduate research assistant at Princeton University. Based on the observation that each laser beam sweeps out planes of light across the detector array, perpendicular sweep axes are used to yield position information independent of the laser beacon orientation. Referring to figure 30, the following equations are obtained.

$$\hat{R} = \frac{1}{n}(\hat{v}_a \times \hat{v}_b)$$

$$R^2 = u + \sqrt{u^2 - r_a^2 r_b^2 (1 - (v_a \cdot v_b)^2)}$$

where

$$n = |\hat{v}_a \times \hat{v}_b|$$

$$u = (r_a^2 + r_b^2)/2$$

Appendix A contains the derivation of these equations, which, when programmed into a microprocessor, are faster than transcendental functions and do not rely on the beacon orientation.

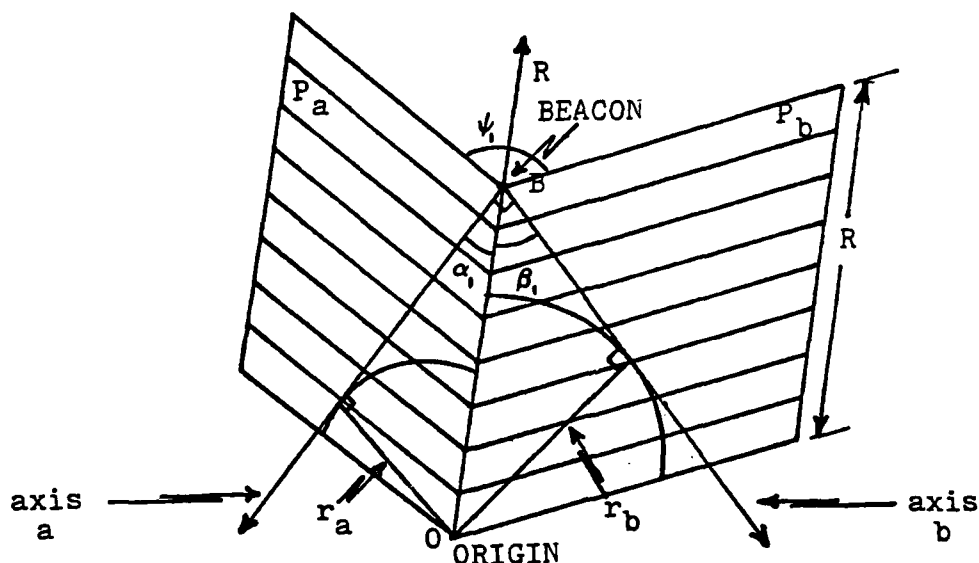


Figure 30: Laser Beam Plane Geometry for Relative Position Calculations

5.4 FUNDAMENTALS OF THE ARRAY DESIGN

The three-dimensional detector array will be placed on the tail of the YO-3A. It is to be designed with respect to size, weight, and strength considerations. Due to the YO-3A's weight limitations, every pound placed on its tail must be countered with five pounds placed forward of the center of gravity. Consequently, the array size must be minimized. On the other hand, however, the array must be large enough to minimize the shadowing of the laser beams on individual detector entrance apertures. Also, the distance

between each detector cannot be too small, or the interval measurements will begin to degrade and accuracy will be lost. In addition, the array has to be sturdy enough to hold each detector securely in place while the aircraft is in flight. Fluctuations in the detectors' relative positions with respect to one another yield errors in the position calculations. Consequently, array size optimization needs to be examined thoroughly.

5.5 TWO-DETECTOR TESTING

Because size is such an important factor in the detector array design, tests were conducted to determine the optimum distance between individual detectors.

For the tests, the laser beacon was set up in direct sunlight approximately 30 meters from two detectors (with 30 Angstrom filters placed inside the detectors). Initially, the detector array was at a zero incidence angle with respect to the beacon, and the spacing between the two detectors was varied from 1.2 meters to 0.15 meter. The time interval resulting from the laser beam sweeping past the detectors was then recorded by a digital timer. Sets of 25 time interval measurements were recorded for various detector separation distances, and a mean, a standard deviation, and a percent error from the mean (standard deviation divided by the mean) were calculated for each set of data. Figure 31 illustrates the results of this set of tests.

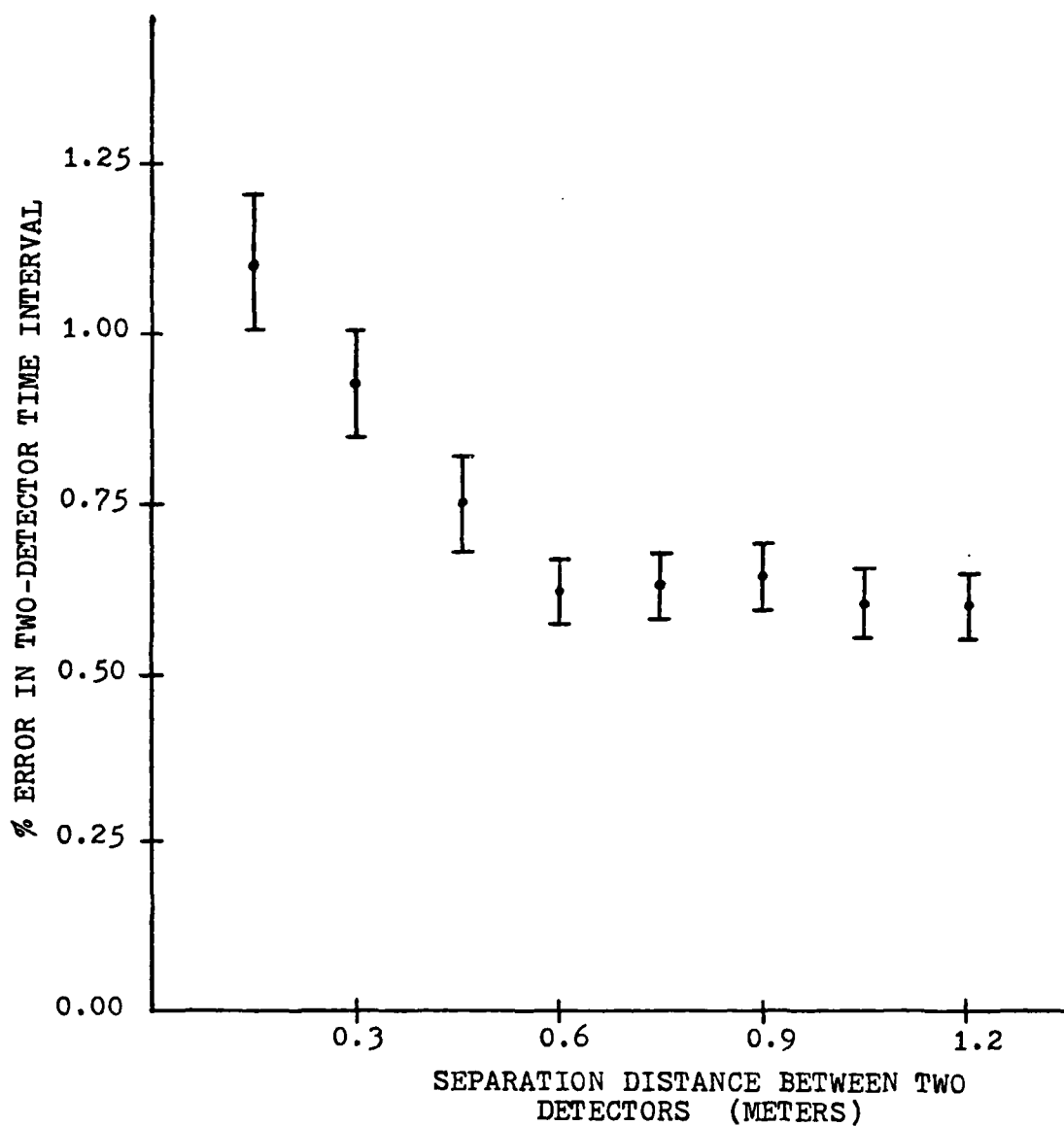


Figure 31: Plot of Time Interval Errors from the Mean as a Function of the Separation Distance Between Two Detectors

As anticipated, below a separation distance of approximately 0.5 meters, the accuracy in the time interval meas-

urements decreased dramatically. This implies that small separation distances yield significant random errors due to the laser beacon's synchronous motor fluctuations. In addition, as the time intervals become small, a tiny difference in the threshold setting--which corresponds to an error in the trigger for the digital pulse--introduces a comparatively large error in the time interval measurement. Above a separation distance of 0.5 meters, these errors decreased in significance, and the accuracy in the time interval measurements increased to a rather constant value (about 0.6 percent). Thus, from an accuracy standpoint, the distance between each detector should not be less than 0.5 meters.

A second set of tests was undertaken to determine if the relative separation distance between the two detectors affected the time interval measurement accuracy as the incidence angle between the laser beacon and the perpendicular to the line joining the detectors was varied. The detector separation distance was chosen to be 0.9 meters, and the detectors were set up on a rotary base. The incidence angle was varied and the time intervals were recorded for the different angles.

Examining the results of this experiment, as seen in figure 32, it appears that the relative distance between the detectors does not influence the accuracy of the time interval measurements. If the results from the previous experiment were to be followed, the accuracy should have begun to

degrade above a 56 degree incidence angle, since a relative separation distance of 0.5 m corresponds to an incidence angle of 56 degrees when the detectors are separated by 0.9 m. However, this is not the case, as the accuracy of the time interval measurements did not depend on the relative distance between the detectors. In reality, degradation in the time interval accuracy above a 75 degree incidence angle was instead due to the detectors missing pulses from the laser sweeps.

The results also reveal a wide variance in the accuracy of the time interval measurements as the incidence angle is changed. Below an incidence angle of 75 degrees, the error from the mean varies from 0.7 percent to about 0.4 percent. However, as long as the percent error remains below approximately one percent of the mean, the system is deemed to be within the accuracy constraints for the project.

In a related test, the separation distance between the two detectors was reduced to 0.6 meters, and the above experiment was again performed. However, this time the accuracy steadily decayed with increasing incidence angle. Consequently, it appears that, above a detector separation distance of approximately 0.6 meters, as the incidence angle varies, the relative distance between the detectors has a negligible effect on the accuracy of the time interval measurements.

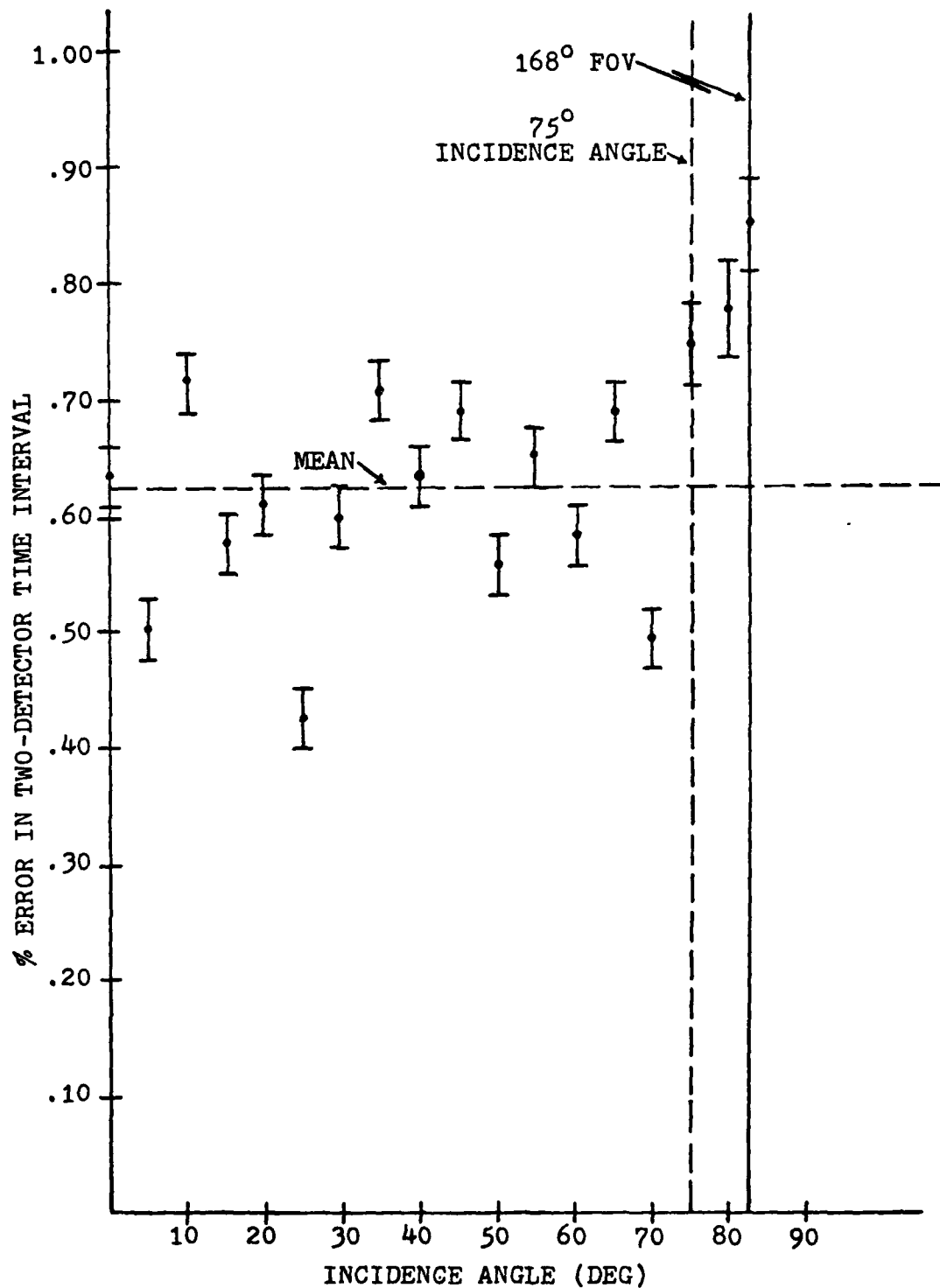


Figure 32: Plot of Time Interval Errors from the Mean as a Function of the Detector Incidence Angle to the Beacon Axis

Based on the above results, the separation distance between individual detectors was chosen to be 0.9 meters for the field tests. This distance was deemed to be optimum due to the negligible effect on the time interval accuracy with varying incidence angles. At the same time the array size was minimized without introducing potentially significant shadowing problems.

5.6 ARRAY CONSTRUCTION

The requirements for a detector array to be used in the field tests include the mounting of four detectors on a solid base with the capability of repositioning the individual detectors. Array weight and size are not critical factors since the purpose of the initial field tests is to determine the operational status of the laser beacon system.

Consequently, the array built for the flight tests consists of 4 aluminum tubes, each 31.75 mm in diameter, arranged in a tetrahedral fashion such that the tubes are mutually perpendicular to each other. The array is secured to a solid base and each detector is attached to its respective tube by a metal mount. The mounts are constructed so that all the detectors point in the same direction. In addition, the mounts can be repositioned to change the distance between the detectors. The initial field tests will be conducted with a distance of 0.9 m separating individual detectors.

For future field tests, and prior to the flight tests, the final array will be built. This array will be constructed of thin, lightweight tubing, probably like the type found in competition bicycle frames, and the detectors will be securely fastened to the ends of the tubes. The array will have the capability to be attached to the tail of the YO-3A.

5.7 SUMMARY

The detector array to be used in the initial field tests is constructed of aluminum tubes arranged in a tetrahedral fashion. The optical detectors attached to the tubes are mutually perpendicular to each other, and they are separated by a distance of 0.9 m.

Two detector array testing indicates that above a detector separation distance of 0.6 m, the relative distance between the detectors with a varying incidence angle has a negligible effect on the accuracy of the time interval measurements. A 0.9 m separation distance was chosen for the initial field tests in order to minimize possible effects of shadowing.

Chapter VI

CONCLUSIONS

This thesis has presented a review of the development, to date, of a laser beacon system which will be used to determine the relative position between two aircraft. Specifically, the relative range, elevation, and azimuth between an observation aircraft and a test helicopter will be calculated with a high degree of accuracy. The emphasis of this paper has been placed on the development of the laser beacon, the detector optics and associated electronics, and the detector array.

The beacon system provides for an apparatus to detect laser beams in the presence of background solar interference through spectral filtering of the incident light and electronic filtering of the photodiode pulses. The laser beacon consists of two rotating fan-shaped narrow width laser beams with wide fields of view. The beams sweep past an array of four detectors which transmit pulses to the electronics package. Compound parabolic concentrators are used as the optical detectors to achieve wide-angle viewing. Thirty Angstrom filters, placed inside the detectors, filter out background solar interference. The detected pulses pass through filters in the electronics system, and are then sent

as digital pulses to the microprocessor for signal processing. Initial tests of the system components demonstrate the potential for their use in aircraft as elements of a relative position measurement system.

AD-A107 973

AIR FORCE INST OF TECH WRIGHT-PATTERSON AFB OH
AIRCRAFT POSITION MEASUREMENT USING LASER BEACON OPTICS.(U)
1981 S 6 WEBB
AFIT-CI-81-58T

F/G 17/7

UNCLASSIFIED

NL

2 OF 2

AD-A107 973



END

DATE

FILED

11-84

DTIC

1.0

2.8 2.5

3.2 2.2

3.6 2.0

4.0 1.8

1.1

1.8

1.25

1.4

1.6

VERACITY RESOLUTION TEST CHART
1963-A

REFERENCES

1. Boxwell, D. A. and Schmitz, F. H., 'Full-Scale Measurements of Blade-Vortex Interaction Noise.' AIAA Paper 80-1009, June 1980.
2. Miles, R. B., 'Laser Beacon System for Aircraft Collision Hazard Determination.' Applied Optics, Vol. 19, p. 2098, July 1980.
3. Military Standardization Handbook, Optical Design, MIL-HDBK-141. Washington D. C. Defense Supply Agency, 5 October 1962.
4. Jenkins, F. A. and White, H. E., Fundamentals of Optics. New York, McGraw-Hill Book Company, Inc., 1957.
5. Lerner, R. M., 'Limitations in the Use of Dielectric Interference Filters in Wide Angle Optical Receivers.' Applied Optics, Vol. 10, p. 1914, 1971.
6. Rabl, A., 'Comparison of Solar Concentrators.' Solar Energy, Vol. 10, p. 93, 1976.
7. Winston, R., 'Light Collection Within the Framework of Geometrical Optics.' J. Optical Society of Am., Vol. 60, p. 245, 1970.
8. Welford, W. T., Optics of Nonimaging Concentrators. New York, Academic Press, 1978.
9. Bracewell, R. N., The Fourier Transform and its Applications. New York, McGraw-Hill Book Company, Inc., 1978.
10. Senturia, S. D. and Wedlock, B. D., Electronic Circuits and Applications. New York, John Wiley and Sons, 1975.
11. Kaplan, M. H., Modern Spacecraft Dynamics and Control. New York, John Wiley and Sons, 1976.

Appendix A

DERIVATION OF THE POSITION DETERMINATION EQUATIONS

The derivation of the position determination equations, accomplished by G. Russell at Princeton University, takes advantage of the observation that the laser beacon sweeps out planes of light across the detector array.

Detectors are located at the origin, 0, and at equal distances 1 along each coordinate axis, x, y, and z (figure 33). Define three time intervals, τ_x , τ_y , and τ_z as the times between the crossing of detector D_0 and the crossing of the respective detectors D_x , D_y , and D_z by the light plane. The time interval is negative in value if that particular axis detector is crossed before the origin detector.

The time intervals are each proportional to the inner product of the respective coordinate unit vectors with the direction of the travel vector defined by the perpendicular to the light plane. Thus, the direction of the travel vector may be recovered in the coordinate system of the array as

$$\hat{v} = \frac{1}{T}(\tau_x \hat{i} + \tau_y \hat{j} + \tau_z \hat{k})$$

where T is the normalizing factor such that

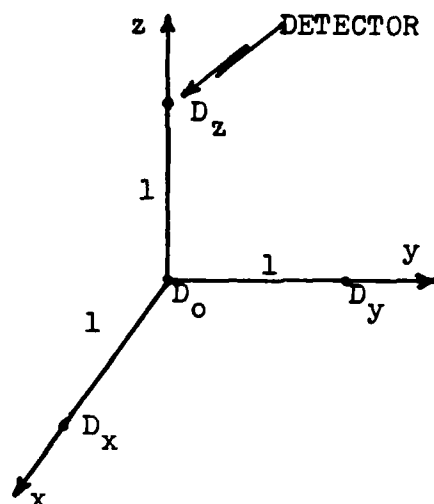


Figure 33: Detector Array Configuration

$$T^2 = r_x^2 + r_y^2 + r_z^2$$

The magnitude of T is related to the perpendicular distance to the sweep axis, r , by the equation

$$r = \frac{1}{\omega} \left(\frac{1}{T} \right)$$

where ω is the sweep rate (for a small $1/r$ ratio)

The direction of the travel vector \hat{v} and the distance to the axis, r , are the only information which can be ascertained from a single sweep. This restricts the sweep axis to lie tangent to a circle of radius, r , around the origin and in the plane perpendicular to \hat{v} .

These parameters are obtained for each sweep axis, and are being subscripted 'a' and 'b' for the respective axes (figure 34).

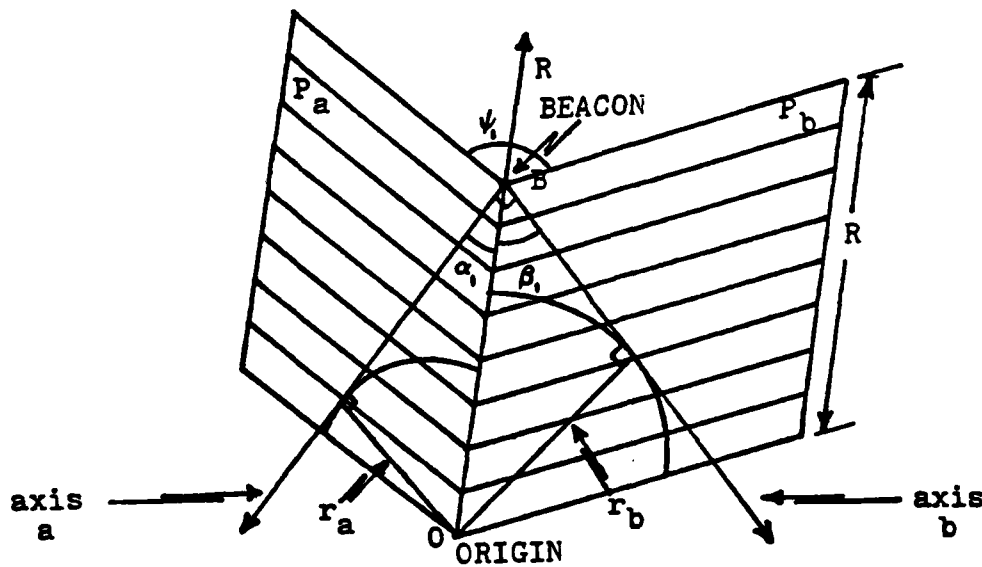


Figure 34: Beam Plane Geometry for Relative Position Calculations

The laser beacon is designed to have exactly perpendicular sweep axes. This information is used in the ensuing calculations.

The two vectors \hat{v}_a and \hat{v}_b define two planes. The planes are perpendicular to their respective vectors and each includes the origin. The beacon axes must lie one in each of

these planes, implying that the beacon lies somewhere along the line of intersection of the planes. This line is defined by

$$\hat{R} = \frac{1}{n}(\hat{v}_a \times \hat{v}_b)$$

with $n = |\hat{v}_a \times \hat{v}_b|$ to normalize R

The distance from the origin to the beacon is determined in the following manner.

Consider the two planes which are perpendicular to the vectors \hat{v}_a and \hat{v}_b . These two planes intersect at an oblique angle, ψ_1 , which is defined by the equation

$$\cos \psi_1 = -|\hat{v}_a \cdot \hat{v}_b|$$

where $||$ indicates an absolute value

Define also the angle of intersection of each sweep axis with the vector R on which the beacon lies. This means that the angle α_1 corresponds to the intersection of R and the axis 'a' while the angle β_1 corresponds to the intersection of R and the axis 'b'. Note that these angles have the relationships

$$\sin \alpha_1 = \frac{r_a}{R}$$

$$\sin \beta_1 = \frac{r_b}{R}$$

where R is the distance from the origin to the beacon

Since the laser axes are mutually perpendicular, two points, each located one unit from the beacon along their respective axes, are separated by a distance $\sqrt{2}$ (see figure 35). The distance between these two points can be expressed in terms of the angles α_1 , β_1 , and ψ_1 by dividing the distance into perpendicular segments, as shown. Thus,

$$s^2 = (a + d)^2 + b^2 + c^2$$

Substituting α_1 , β_1 , and ψ_1 yields

$$s^2 = (\sin\beta_1 + \sin(\psi_1 - \frac{\pi}{2})\sin\alpha_1)^2 + (\cos\alpha_1 - \cos\beta_1)^2 \\ + (\cos(\psi_1 - \frac{\pi}{2})\sin\alpha_1)^2$$

Since $\sin\alpha_1 = r_a/R$ and $\sin\beta_1 = r_b/R$, the following results:

$$s^2 = \left[\frac{r_b}{R} - \frac{r_a}{R} \cos\psi_1 \right]^2 + \left[\sqrt{1 - \left(\frac{r_a}{R}\right)^2} - \sqrt{1 - \left(\frac{r_b}{R}\right)^2} \right]^2 + \left(\frac{r_a}{R}\right)^2 \sin^2\psi_1$$

Expanding,

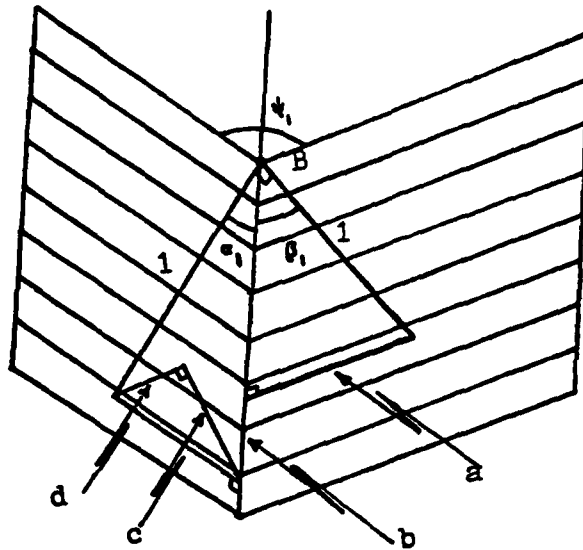


Figure 35: Plane Distance Geometry for Relative Distance Calculations

$$s^2 = \frac{1}{R^2} \left[(r_b^2 + r_a^2 \cos^2 \psi_1 - 2r_a r_b \cos \psi_1) + \left\{ (R^2 - r_a^2) + (R^2 - r_b^2) - 2\sqrt{R^4 - (r_a^2 + r_b^2)R^2 + r_a^2 r_b^2} \right\} + r_a^2 \sin^2 \psi_1 \right]$$

This reduces to

$$s^2 R^2 = 2 \left\{ R^2 - r_a r_b \cos \psi_1 - \sqrt{R^4 - (r_a^2 + r_b^2)R^2 + r_a^2 r_b^2} \right\}$$

Now, since $s^2 = 2$, the equation becomes

$$r_a r_b \cos \psi_1 = -\sqrt{R^4 - (r_a^2 + r_b^2)R^2 + r_a^2 r_b^2}$$

Squaring,

$$R^4 - (r_a^2 + r_b^2)R^2 + (1 - \cos^2 \psi_1)r_a^2 r_b^2 = 0$$

Simplifying this equation and noting that the minus sign in the resulting quadratic can be dropped since

$$r_a, r_b \leq R \leq \sqrt{r_a^2 + r_b^2}$$

results in an equation of the form

$$R^2 = \frac{r_a^2 + r_b^2}{2} + \sqrt{\left(\frac{r_a^2 + r_b^2}{2}\right)^2 - r_a^2 r_b^2 (1 - \cos^2 \psi_1)}$$

Let $u = (r_a^2 + r_b^2)/2$, and because $\cos \psi_1 = -|\mathbf{v}_a \cdot \mathbf{v}_b|$, the following results

$$R^2 = u + \sqrt{u^2 - r_a^2 r_b^2 (1 - (\hat{\mathbf{v}}_a \cdot \hat{\mathbf{v}}_b)^2)}$$

These equations completely specify the position vector R , except for ambiguity in direction, which can be easily resolved. The derivation has the advantage that it results in

equations which do not use transcendental functions and are independent of the laser beacon orientation.